COLEBROOKEA OPPOSITIFOLIA STEM EXTRACT AS GREEN CORROSION INHIBITOR FOR MILD STEEL IN 1 M HCl SOLUTION

A DISSERTATION WORK SUBMITTED
FOR THE PARTIAL FULFILLMENT OF THE
REQUIREMENTS FOR THE
MASTER OF SCIENCE DEGREE IN CHEMISTRY

SUBMITTED BY:

Name: Dipak Pandey

T.U. Examination Roll No.: CHE 1876/076

T.U. Registration No.: 5-2-33-226-2015

SUBMITTED TO:

DEPARTMENT OF CHEMISTRY

AMRIT CAMPUS

INSTITUTE OF SCIENCE AND TECHNOLOGY

TRIBHUVAN UNIVERSITY, KATHMANDU, NEPAL

September, 2023

BOARD OF EXAMINER AND CERTIFICATE OF APPROVAL

This project work entitled **"*Colebrookea oppositifolia* stem Extract as Green Corrosion Inhibitor for Mild Steel in 1 M HCl Solution"** by Mr. Dipak Pandey under the supervision of Asst. Prof. Sanjay Singh, Department of Chemistry, Amrit Campus, Tribhuvan University, Kathmandu, Nepal, and under co-supervision of Asst. Prof. Hari Bhakta Oli, Department of Chemistry, Amrit Campus, Tribhuvan University, Kathmandu, Nepal, hereby submitted has been approved for partial fulfillment of the requirement for completion of his Master of Science (M.Sc.) Degree in Chemistry.

.....

Supervisor

Asst. Prof. Sanjay Singh

Department of Chemistry

Amrit Campus, TU, Kathmandu, Nepal

.....

Co-Supervisor

Asst. Prof. Hari Bhakta Oli

Department of Chemistry

Amrit Campus, TU, Kathmandu, Nepal

.....

Internal Examiner

Asst. Prof. Dr. Deval Prasad Bhattarai

Department of Chemistry

Amrit Campus, TU, Kathmandu, Nepal

.....

External Examiner

Prof. Dr. Jagadeesh Bhattarai

Central Department of Chemistry

Tribhuvan University, Kathmandu, Nepal

.....

M.Sc. Chemistry Coordinator

Assoc. Prof. Dr. Bhushan Shakya

Department of Chemistry

Amrit Campus, TU, Kathmandu, Nepal

.....

Head of the Department

Assoc. Prof. Kanchan Sharma

Department of Chemistry

Amrit Campus,TU, Kathmandu, Nepal

Date: Sept 29, 2023

LETTER OF RECOMMENDATION

This is to recommend that the dissertation work entitled, "*Colebrookea oppositifolia* stem Extract as Green Corrosion Inhibitor for Mild Steel in 1 M HCl Solution'' has been carried out by Mr. Dipak Pandey as partial fulfilment for the requirements of Master of Science Degree in Chemistry. This is his original work and has been carried out under my guidance and supervision. To the best of my knowledge, this research work has not been submitted to any institutes / universities for any other degree.

.....

Supervisor

Asst. Prof. Sanjay Singh

Department of Chemistry

Amrit Campus,

Tribhuvan University,

Kathmandu, Nepal

Tribhuvan University
Amrit Campus
Department of Chemistry

Date: September, 2023

DECLARATION

I, Dipak Pandey, hereby declare that the work entitled "*Colebrookea oppositifolia* stem Extract as Green Corrosion Inhibitor for Mild Steel in 1 M HCl Solution" submitted to Institute of Science and Technology Tribhuvan University as partial fulfilment for the requirements of Master of Science Degree in Chemistry has been done by myself and has not been submitted earlier in part or full in this or any other form to any other university/institute, here or elsewhere for the award of any degree. All sources of information have been specifically acknowledged by reference to the authors or institutions.

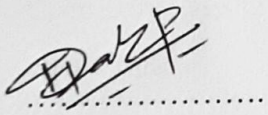

Dipak Pandey

Date: September, 2023

ACKNOWLEDGEMENTS

I am initially expressing my profound gratitude and respect to my supervisor, Asst. Prof. Sanjay Singh and Co-supervisor, Asst. Prof. Hari Bhakta Oli for their continuous support, ideas, motivation, and knowledgeable advice throughout my research. Their guidance and suggestions had been the key for successful completion of this thesis.

I would also like to thank Assoc. Professor Kanchan Sharma, Head of Department of Chemistry, Amrit Campus, and Assoc. Professor Dr. Bhushan Shakya, Co-ordinator of M.Sc. Program, Department of Chemistry, Amrit Campus.

I want to express my sincere thanks to Prof. Dr. Amar Prasad Yadav and Asst. Prof. Anju Kumari Das for their assistance with the polarization measurement at Central Department of Chemistry, Tribhuvan University.

I am thankful to Mani Raj Budhathoki and Nanda Krishna Manandhar, who helped me by providing required instruments. I am also thankful to faculties, administrative staffs and technicians of Chemistry Department, for giving kind support during the research work.

Finally, I am heartily thankful to my family, friends, and contemporaries of M.Sc. Chemistry, Bishnu Pandey and Devashish Karn for their great support and co-operations.

Dipak Pandey
Sept 2023

ABSTRACT

The inhibitive performance of *Colebrookea oppositifolia* stem extract was examined as a green corrosion inhibitor for mild steel in 1 M HCl medium by weight loss tests, potentiodynamic polarization (PDP), and electrochemical impedance spectroscopy (EIS). The extract was characterized by UV and FTIR spectroscopic test. The kinetic and thermodynamic parameters have also been calculated and discussed. Based on the weight loss measurement remarkable inhibition efficiency of 90.34% was achieved. Electrochemical measurements showed an inhibitory effect of up to 77.18%. The EIS analysis results showed that the increase in inhibitor concentration led to a significant increment of charge transfer resistance via adsorption of inhibitors at the metal/solution interface. The adsorption of inhibitor molecules on the surface of mild steel followed a Freundlich adsorption isotherm.

Keywords: *Colebrookea oppositifolia Mild Steel, Green corrosion Inhibitor, Weight Loss, Polarization, Impedance, Adsorption.*

शोधसार

अम्लद्वारा गरिने सफाइपछि स्टिलको सतहमा हुने थप क्षयीकरणलाई कम गर्न धुर्सेलीको डाँठको नीकासीलाई हरित निषेधकको रुपमा प्रयोगगरि यसको निषेधकीय क्षमताको अध्ययन तौल मापन विधि तथा विद्युत रसायनिक विधिबाट गरिएको छ। निकासिको चारित्रिक अध्ययन प्रकाशिय वर्णपट विधिबाट गरिएको छ। तौल मापन तथा विद्युत रसायनिक विधिबाट गरिएको अध्ययन अनुसार हरित निषेधकको निषेधकिय क्षमता क्रमशः ९०.३४ र ७७.१८ % पाइएको छ। हरित निषेधकको अवशोषण अध्ययन गर्दा फ्रेन्डलिक समताप रेखा अनुरुप रहेको पाइएको छ।

Keywords: *Colebrookea oppositifolia Mild Steel, Green corrosion Inhibitor, Weight Loss, Polarization, Impedance, Adsorption.*

LIST OF ABBREVIATIONS

Ω	Ohm
Θ	Fraction of Surface Coverage
C_{inh}	Corrosion Inhibitors
CR	Corrosion Rate
C_{dl}	Double-layer Capacitance
E_a	Activation Energy
E_{corr}	Corrosion Potential
EIS	Electrochemical Impedance Spectroscopy
FTIR	Fourier Transform Infrared Spectroscopy
GDP	Gross Domestic Product
HOMO	Highest Occupied Molecular Orbital
I_{corr}	Corrosion Current
IE	Inhibition Efficiency
LUMO	Lowest Unoccupied Molecular Orbital
MS	Mild Steel
OCP	Open Circuit Potential
PDP	Potentiodynamic Polarization
SCE	Saturated Calomel Electrode
UV	Ultra Violet
ppm	Parts Per Million

LIST OF TABLES

LIST OF FIGURES

TABLE OF CONTENTS

CHAPTER 1
INTRODUCTION

1.1. Background

Corrosion is a naturally occurring electrochemical reaction that involves the conversion of a refined metal into one of its more chemically stable compounds, usually an oxide, a hydroxide or sulfide. This chemical transformation occurs as the metal reacts with its surrounding environment, leading to the gradual deterioration in the properties of metal over a period of time where anodic and catholic reactions take place (Olasunkanmi & Ebenso, 2020). As corrosion is a devastating phenomenon, it is causing huge economic losses in the world. Based on NACE report, It is estimated that about 3.4% of GDP of developed countries is being lost due to corrosion worldwide (Koch et al., 2016). Among all corrosion cases, corrosion in mild steel (MS) is to be extensively studied and protection methods to be applied. It is because, the MS (an iron alloy with a low carbon content ranging from 0.05% to 0.25%, along with manganese, phosphorus, and sulphur) is one of the world's most extensively consuming alloy in the industrial areas due to its excellent mechanical properties, weldability, and affordable purchasing costs (Kong et al., 2022). Though it has great application potential but prone to corrosion especially in acid cleaning processes where strong acids are used and hence imparts huge economic loss. Thus, researchers have been passionate about investigating efficient, energy-saving, and eco-friendly metal anti-corrosion techniques (Nadi et al., 2019).

In acid electrolytic medium oxidation (dissolution of metal/alloys) takes place at anode and evolution of hydrogen as well as oxygen reduction takes place at cathode of the corrosion cell which is represented as.

i. Oxidation (Dissolution of metal/alloys at anode).

   $M(s) \longrightarrow M^{n+}(aq.) + ne^-$

ii. Reduction (Oxygen Reduction at cathode in acidic medium).

   $O_2(g) + 4H^+ + 4e^- \longrightarrow 2H_2O(l)$

iii. Hydrogen evolution from acidic Medium.

   $2H^+ + 2e^- \longrightarrow H_2(g)$

The overall reaction is represented as,

$$M(s) + nH^+ \longrightarrow M^{n+}(aq) + H_2(g)$$

Where, M = Fe (metal/ alloy) & n = number of electrons (Hou et al., 2017).

Indeed, the use of inhibitors are needed to minimize corrosion in descaling, acid pickling like processes (Roberge, 2019). A corrosion inhibitor is a chemical compound that is used to slow down or prevent the corrosion of metal in the various corrosive environments. Corrosion inhibitors forms a barrier over the surface of the metal/alloy, which prevents it from coming into contact with the corrosive agents.

1.2. Types of Corrosion inhibitors

Inhibitor is a substance that is added into metal in order to either prevent or retard the corrosion process. Corrosion inhibitors work by forming a protective layer on the metal surface, which acts as a barrier against corrosive agents such as moisture, oxygen, and other environmental factors. This protective layer can be formed either through a chemical reaction with the metal surface or through adsorption onto the surface (Palanisamy, 2019). Common types of corrosion inhibitors are listed here.

1.2.1. Anodic inhibitor

An anodic inhibitor is a type of corrosion inhibitor that specifically works by reducing or slowing down the oxidation reaction at the anode during a corrosion process by forming a passive layer on the metal surface. Chromates, nitrates, phosphate, and permanganates are some examples of anodic inhibitors. In highly aggressive or acidic environments, anodic inhibitors may not provide adequate protection. They are generally more effective in milder or less corrosive conditions (Yamamoto et al., 2019).

1.2.2. Cathodic inhibitor

A cathodic inhibitor is a type of corrosion inhibitor that slows down or hinders the reduction reaction occurring at the cathode during a corrosion process by limiting the diffusion of reducing species to the metal surface. Some elements like As, Bi, and Sb are considered as cathodic poisons that reduces the rate of corrosion by decreasing hydrogen evolution rate. Also, when oxygen is removed from corrosive media, the rate of corrosion is found to be decreased. Cathodic inhibitors are such inhibitors which when added to the corrosive system shifts the potential more towards anodic direction (Touhami et al., 2000). In this process, the metal ions i.e, cations are transported towards cathode and are precipitated chemically and electrochemically which blocks the metal surface from attacking media (Palanisamy, 2019). However, certain cathodic inhibitors may include harmful materials, necessitating cautious handling and disposal

to reduce their environmental effects. Meanwhile, cathodic protection systems demand continuous monitoring and upkeep to maintain their efficiency. Maintenance of electrical components may be necessary over time (Mouanga et al., 2015).

1.2.3. Synthetic organic inhibitor

An organic corrosion inhibitor that are prepared from synthetic organic compounds and used in order to retard or completely prevent the corrosion reactions occurring on the metal surfaces on both the anodic and cathodic areas of metal surface. Examples of organic corrosion inhibitors include amine derivatives, carboxylates, imidazolines, and green inhibitors. Synthetic organic inhibitors have potential uses in various industrial purposes such as oil and gas, automotive, aerospace, marine, power plants, and electronics to protect metal equipment and structures from corrosion in various corrosive environments. However, they are limited by their potential for compatibility issues, the tendency to degrade over time, and cost-related factors (Ahmed et al., 2018).

1.2.4. Green corrosion inhibitor

Green corrosion inhibitors are biodegradable, environmentally friendly compounds that are added to metals or alloys to prevent or reduce their corrosion. These inhibitors form a protective layer on the surface of metal to be protected, and eventually prevents the exposure of metal to the corrosive media. Examples of green corrosion inhibitors include plant extracts, biopolymers, organic compounds, and nanoparticles. They are commonly used in various industries such as oil and gas, marine, aerospace, and construction (Verma, 2021).

Plant extract constituents of phytochemicals such as alkaloids, flavonoids, polyphenols, tannins, nitrogen bases, phenolic, carbohydrates that contain N, S, P and O as well as triple or double conjugate bonds that are the major interacting sites for the phytochemicals to get adsorbed on the MS surface.

1.3. *Colebrookea oppositifolia* stem as a green corrosion inhibitor

C. oppositifolia is one of the commonly available evergreen perennial shrubs plants in the Himalayan region of Nepal (Palpa, Syangja, Gulmi). The phytochemical screening of tests *C. oppositifolia* indicated the presence of alkaloids, flavonoids, glycosides, steroids and saponins, terpenoids, tannins, and cardiac glycosides as main phytocompounds (Ajaib et al., 2018).

The primary chemical constituents isolated from the extract Acteoside , Gallic acid, Chrysin, Negletein-6-beta-d-glucopyranoside, 5,7,2′-trihydroxyfa-vone 2′-O-beta-D-glucopyranoside (Viswanatha et al., 2021).

Taxonomic Classification:

Kingdom: Plantae

Division: Tracheophyta

Order: Lamiales

Family: Lamiaceae

Genus: *Colebrookea*

Species: *oppositifolia*

Figure 1: *Colebrookea oppositifolia plant*

The presence of lone pairs of electrons and π-electrons in plant extract can lead to the formation of a protective layer on metal surfaces. This property can be utilized in the development of green inhibitors, which are becoming increasingly popular due to their sustainability and eco-friendliness.

1.4. Role of Phytochemicals for protective barrier film on MS surface

Phytochemicals contain hydroxyl, carboxylic, and amino functional group having oxygen, nitrogen, and sulphur heteroatoms that allows them to interact with metal surfaces and form a protective barrier film on metal surfaces by adsorbing onto the surface and forming a stable film. The stable film formed acts as a barrier towards the corrosive medium, thus inhibiting corrosion. Phytochemicals offer a sustainable and eco-friendly alternative to traditional synthetic inhibitors (Bhardwaj et al., 2021).

1.5. Objectives of the study

1.5.1. General objectives

The general objectives of the work is to extract the phytochemical from *Colebrookea oppositifolia* stem and to study its corrosion inhibition efficiency on mild steel in 1 M HCl solution.

1.5.2. Specific objectives

Specific objectives of this study are:

1. To prepare the extract of *Colebrookea oppositifolia* stem powder using methanol.
2. To use the extract as a green inhibitor in acid solution for different concentrations.
3. To carry out weight loss, polarization, and EIS measurements.
4. To study the inhibition efficiency and thermodynamic parameters of methanol extract solution in 1 M HCl.

CHAPTER 2
LITERATURE REVIEW

Various plant extracts or biodegradable organic materials are used as green inhibitors to prevent corrosion of mild steel in the acid medium due to easy accessibility, eco-friendly on earth, and non-toxic in nature. Various mechanisms of action have been proposed for the corrosion inhibition property of natural products. Based on these studies, concluded that green corrosion inhibitor forms compact barrier film via physisorption or chemisorption onto the metal-solution interface by removing molecules of water from it (Finšgar & Jackson, 2014). The formation of a coordinate covalent bond through interaction between the vacant d-orbital of the Fe atom and the lone pair and -electrons present in the molecules of GCIs (Ahamad et al., 2010).

Odewunmi et al., (2015) was investigated the corrosion inhibition efficiency of methanol extract of Watermelon rind (*C. lanatus*) for mild steel corrosion in hydrochloric acid (HCl) solution by using weight loss, potentiodynamic polarization, and electrochemical impendence techniques. The inhibition efficiency increases with an increase in concentration (90.20% at the highest concentration 1000 ppm) and decreases with an increase in temperature.

Marsoul et al., (2020) used pomegranate bark (*Punica granatum L*) extract as GCI for mild steel in HCl solution by using the EIS method. The Nyquist plots of different concentrations of bark extract in 1 M HCl revealed the role of charge transfer process on the corrosion of that system. In addition, a larger radius of the capacitive loop with a higher concentration of inhibitor indicated that the efficiency of the extract is increased due to the increase of energy barrier for corrosion. Additionally, the impedance is decreased with an increased temperature as the inhibitor molecules get desorbed from the protective layer that elucidated the rate of corrosion is increased.

The corrosion inhibition efficiency of *Mahonia nepalensis* extract was investigated by Karki et al., (2021). The extract has been evaluated as a corrosion inhibitor for mild steel in 0.5 M H_2SO_4 solution by means of gravimetric, potentiodynamic polarization technique. According to electrochemical parameters results the extract acted as an efficient mixed type inhibitor. The adsorption of the inhibitor on mild steel surface was followed the Langmuir adsorption isotherm. SEM and EDX techniques confirmed the adsorption of the extracts on steel surface.

Bahlakeh et al., (2019) investigated the inhibitive action of the seed extract of *Peganum harmala* in 1 mol/L HCl solution using electrochemical measurement that revealed a mixed anodic/cathodic type inhibition behavior, reaching a maximum efficiency of 95% by using 800 ppm of the extract in which a noticeable shift of both cathodic and anodic branches to smaller corrosion current densities was observed.

***Table 1**: Literature review of different plants and their parts on corrosion inhibition study*

S. N.	Plant name	Plant part	Solvent	Concentration	Medium	Method	Efficiency (%)	*Reference*
1.	Ginger	root	CH_3OH	200 ppm	1M HCl	WLM PDP EIS	95.00 92.30 90.60	Gadow & Motawea, (2017)
2.	*Acacia catechu*	bark	H_2O	600 mg/L	0.5M H_2SO_4	WLM PDP EIS	93.85 - 93.12	Haldhar et al., (2020)
3.	*Artemisia vulgaris*	stem	CH_3OH	1000 ppm	1M H_2SO_4	WLM PDP	92.58 88.06	Parajuli et al., (2022)
4	*Rhynchostylis retusa*	stem	CH_3OH	1000 ppm	1M H_2SO_4	WLM PDP	87.51 93.24	Chapagain et al., (2022)
5	*Artemisia pallens*	-	CH_3OH	1.5 g/L	4N HCl	WLM PDP	93.00	Kalaiselvi et al., (2010)
6	*Camphor*	leaf	H_2O	600 mg/L	1M HCl	WLM PDP EIS	89.4 87.3	Chen et al., (2020)
7	*Lantana camara*	bark	CH_3OH	1000 ppm	1M HCl	WLM PDP EIS	89.93 97.33	Shrestha et al., (2019)
8.	*Tinospora crispa*	stem	C_3H_6O	1000 ppm	1M HCl	WLM PDP EIS	87.89 78.14	Hussin et al., (2016)
9.	*Murraya koenigii*	leaf	H_2O	600 mg/L	H_2SO_4	WLM/ PDP	94.66 96.66	Quraishi et al., (2010)

2.1. Research Gap

Numerous studies have recently been conducted to evaluate the various plant-based sources as mild steel (MS) corrosion inhibitors in acidic circumstances. The fundamental goal of these studies is to identify the phytochemicals that are responsible

for the excellent inhibitory effects. There is indeed a high possibility that indigenous plants in our country may contain plant extracts with efficient inhibitory properties on MS corrosion. Among them, the plant's phytochemical analysis of *Colebrokea oppositifolia* revealed a potential green inhibitor, there has been no earlier research on its utilization as a mild steel corrosion inhibitor.

In the future, there is a growing emphasis on harnessing compounds found in nature to develop efficient corrosion inhibitors. Natural compounds offer several advantages, including their abundance, eco-friendliness, and potential for low toxicity. By exploring and understanding the chemical properties of natural compounds, researchers can identify and optimize them for effective corrosion inhibition.

CHAPTER 3
MATERIALS AND METHODS

3.1. Collection of Plant and Preparation of Powder

Stems of *Colebrookea oppositifolia* (Dhurseli in Nepali) plant were collected from Darchha Rampur (latitude: 27°82'61.0"N, longitude: 83°94'20.4"E and altitude 1100 m) Palpa, Nepal in September 2022. Collected stem samples were chopped into smaller pieces, and dried for one month in the shade at room temperature. The dried stem was ground into the fine powder with the help of a grinding machine, in Central Department of Chemistry, Kirtipur, Kathmandu,Nepal, and stored in an airtight container.

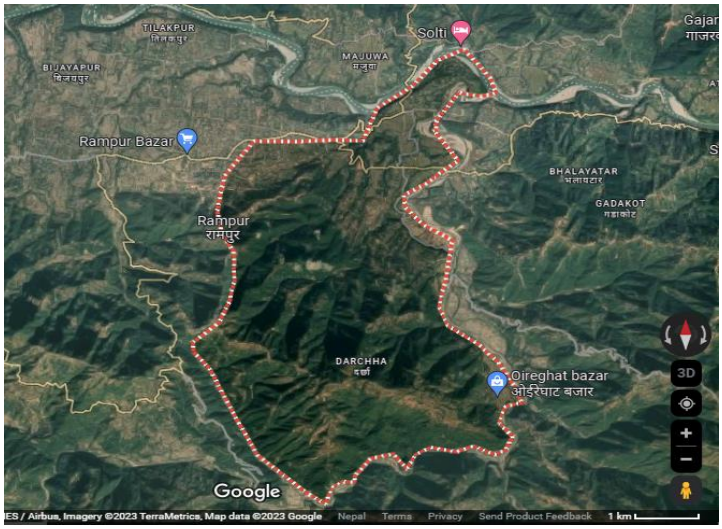

Figure 2: *Google map of plant collected area*

3.2. Preparation of plant extract

About 100 g of prepared powder was soaked in 750 mL methanol for 7 days with occasional shaking. The mixture was then filtered by using an ordinary filter paper. In the residue, methanol was added and previous process was repeated. In order to get all the phytochemical content in plant, this procedure was done several times until a colorless solution was obtained. A digital rotary evaporator (IKA 10) was used to concentrate the filtrate. The concentrated extract was evaporated up to dryness using a Clifton water bath at 40 °C. The dry extract was used as inhibitor in this experiment. Before proceeding experiment, extract was characterized by spectroscopic methods.

3.3. Spectroscopic Test Method

3.3.1. UV-Visible spectroscopic analysis

UV-Vis spectroscopy is a technique that measures the absorption of light in the ultraviolet and visible regions of the electromagnetic spectrum. The spectroscopic characterization of the methanol extract of *Colebrookea oppositifolia* stem was carried out at the department of chemistry, Amrit Campus, Kathmandu, using a Labtronics, LT-2802 double beam ultraviolet-visible (UV-Vis) spectrometer, which served to identify the unsaturation and electron-rich center within the inhibitor molecule. Spectra was recorded in the UV range (200-400nm) with 1 nm scan interval.

3.3.2. FTIR analysis

FTIR spectroscopy is a versatile analytical technique that provides valuable information about the functional groups, π-bond conjugate systems, aromatic and aliphatic structures present in organic compounds. In this experiment, the FTIR spectra of methanol extract were collected using (PerkinElmer Spectrum IR Version 10.6.2) FTIR spectrometer in Amrit Campus, Kathmandu. Spectra was recorded in the range 4000 to 450 cm^{-1} at scan interval 4 cm^{-1}.

3.4. Preparation of corrosive medium

A stock solution of 1M HCl was prepared by diluting 187 mL of concentrated acid (Conc. HCl) in a 2000 mL volumetric flask. The concentration of HCl was confirmed by titrating with 1M Na_2CO_3 solution.

3.5. Preparation of inhibitor solution

Inhibitor stock solution was prepared by dissolving 1 g of methanol extract in 1M HCl solution. The mixture was filtered to remove the undissolved part and the filtrate was transferred to a 1000 mL volumetric flask and 1M HCl was added up to mark. This results in the formation of 1000 ppm of stock solution. Other required concentrations (800, 600, 400, and 200 ppm) of inhibitor solutions were prepared by serial dilution of this stock solution.

3.6. Preparation of mild steel sample

Mild steel sheet (0.15% to 0.25 % of C, 0.25-0.60% Mn, 0.35% Si, 0.05% P, 0.05% S, and the rest of iron) used in this study were collected from Thamel, Kathmandu and coupons of dimension (3.5cm×3.5cm×0.12cm) were made. Each coupon was polished

with #80-1200 grit SiC paper before being rinsed with hexane and stored in moisture-free desiccators. Before each weight loss and electrochemical experiment, each sample was sonicated in ethanol, dried, and its dimensions were recorded.

3.7. Weight Loss Measurement

Weight Loss Measurement was used to examine the inhibition efficiency (IE) of inhibitor solutions. By immersing the MS coupons in acid solutions in the absence and presence of different inhibitor concentrations, different parameters such as the effect of immersion time, the effect of inhibitor concentration on corrosive media, and the influence of temperature were examined. Prior to investigating each effect, the dimensions of each coupon were measured with a Vernier caliper. The weight of the respected samples was measured before and after the conclusion of immersion experiments at the set immersion period, inhibitor concentration, and working temperature. The difference in weight i.e. weight loss data are used to calculate corrosion rate, inhibition efficiency, and surface coverage by inhibitors using the formula in equations (1), (2), and (3) respectively.

$$\text{Corrosion rate (CR)} = \frac{K \times \Delta W}{ATD} \quad \ldots(1)$$

$$\text{Inhibition efficiency (\%)} = \frac{(W_2 - W_1)}{W_2} \times 100 \quad \ldots(2)$$

$$\text{Surface coverage } (\theta) = \frac{(W_2 - W_1)}{W_2} \quad \ldots(3)$$

Where, K =87600 (constant); ΔW= weight loss in grams; A= area in cm^2, D = density in g/cm^3; T= time in an hour; W_1 and W_2 are the weight losses for mild steel in the presence and absence of inhibitor respectively.

3.8. Electrochemical Measurements

3.8.1. Potentiodynamic Polarization

Potentiodynamic polarization method provides useful information about corrosion current (i_{corr}), the corrosion potential (E_{corr}), and Tafel slopes. In this research, electrochemical measurement was carried out in Gamry potentiostat interface 1010 at Central Department of Chemistry, TU, Kirtipur. Potentiodynamic polarization and EIS measurement was performed in a three-electrode setup with mild steel as the working

electrode, graphite as the counter electrode, and saturated calomel electrode as the reference electrode. Both anodic and cathodic polarization in the potential window -0.8 to -0.2 V i.e. ±300 mV from OCP with a scan rate of 1 mV/s was applied for both as-immersed and 1 h immersed conditions.

A typical tafel extrapolation method is based on the mixed potential theory in which intersecting point of anodic and cathodic reactions corresponds to corrosion-current density (I_{corr}) and corrosion potential (E_{corr}). A Tafel plot is a graph of the logarithm of the corrosion current density ($log I_{corr}$) versus the potential (E_{corr}). Tafel curve was used to calculate the Tafel slopes and corrosion current from the solution confined in the 1 cm^2 surface area for each test solution, as well as corrosion inhibition efficiency was calculated using the formula in equations (4).

$$\text{Corrosion inhibition efficiency (IE, \%)} = \frac{I_{corr} - I^*_{corr}}{I_{corr}} \times 100 \qquad \ldots(4)$$

$$\text{Fraction of surface coverage } (\theta) = \frac{I_{corr} - I^*_{corr}}{I_{corr}} \qquad \ldots(5)$$

Where, I_{corr} and I^*_{corr} are the corrosion current in the absence and presence of inhibitor respectively.

3.8.2. Electrochemical Impedance Spectroscopy

EIS data is typically analyzed using Nyquist plots, which are plots of the imaginary component of the impedance (Z_{Img}) versus the real component (Z_{real}). By analyzing the shape and position of semicircular arcs of the Nyquist plot, quantitative parameters such as charge transfer resistance (R_{ct}), double-layer capacitance (C_{dl}), and solution resistance (R_s) can be extracted. These parameters provide information about the electrochemical kinetics, corrosion rate, and corrosion protection effectiveness (Lasia, 2002). Corrosion behavior of Mild steel samples for various concentrations of inhibitors in 1 M HCl at 25 °C was observed by EIS using a 10 mV amplitude AC signal with a frequency range of 100 kHz to 10 mHz was applied for both as-immersed and 1 h immersed conditions as similar corrosion cell mentioned in potentiodynamic polarization part. The diameter of the Nyquist plots was used to compute the charge transfer resistance (R_{ct}), and the inhibition efficiency was determined using the Equation (6) below.

$$\text{Inhibition Efficiency (IE\%)} = \frac{R_{ct} - R_{ct}^{0}}{R_{ct}} \times 100\% \qquad \ldots(6)$$

Where, R_{ct} and R^{0}_{ct} are charge transfer resistances in 1 M HCl + Inhibitor and 1 M HCl, respectively.

The impedance diagrams were analyzed using the Zview software in terms of the equivalent circuit (EC) given in Figure 18. The steel/solution interface dose not behave as ideal capacitor, and thus, one constant phase element (CPE) is applying for fitting the curve with more accuracy.

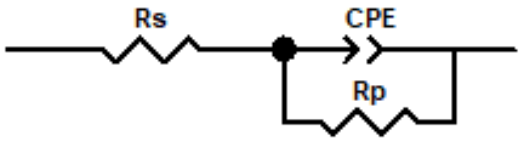

Figure 3: *The equivalent circuit model used to fit the impedance spectra*

Where R_s is solution resistance, R_{ct} is charge transfer resistance at the metal/solution interface and *CPE* is a constant phase element representing the double layer capacitance C_{dl} of the metal/solution interface. The impedance function of CPE is represented by the expression,

$$Z_{CPE} = \frac{1}{Q(jw)^{n}} \qquad \ldots(7)$$

Where, Q represents the magnitude of the CPE, j represents the imaginary root ($\sqrt{(-1)}$), w is the angular frequency (w = 2pf), and n is the deviation index, ($-1 \leq n \leq +1$) it can reflect the heterogeneity of the surface of mild steel (Tan et al., 2021).

CHAPTER 4
RESULTS AND DISCUSSION

4.1. UV-Visible Spectroscopic Measurements

The UV-Visible spectroscopy is an analytical technique which is used for the identification of the presence of lone pair of electrons or conjugated π-electron systems in the organic compounds. In figure 4, the UV-Visible spectra of of methanol extract of *C. oppositifolia,* the sharp peak at 214 nm and 272 nm associated with the presence of lone pairs of electrons, and the unsaturation in the compound. The sharp peak at 214 nm is due to n-π* transition whereas the peak range at 250 to 350 is due to π-π* transition of the inhibitor molecule (Sharma et al., 2021).

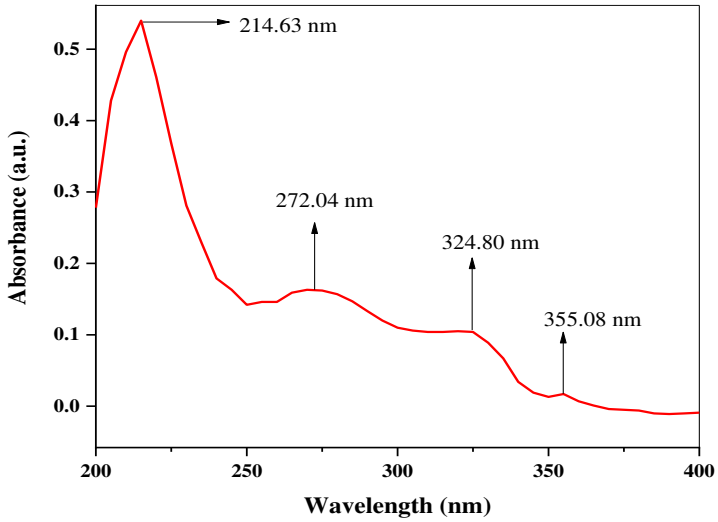

Figure 4: *UV-Visible spectrum of methanol extract of C. oppositifolia*

4.2. FTIR Spectroscopic Measurements

Fourier Transform Infrared Spectroscopy (FTIR) is a fast and non-destructive analytical method which gives information about different functional groups present in the compound with their molecular structure and conformation (Mohamed et al., 2017).

The FTIR spectra of methanol extract is plotted in figure 5. The absorption peaks at around 3262 cm^{-1} indicated the presence of OH groups in the structure (Sharma et al., 2021). Sharp peak at 2924 cm^{-1} is corresponds to C-H stretching of the aromatic ring, the peaks around 1710 cm^{-1} is due to C=O stretch absorption, associated with carbonyl group (Ishtiaq et al., 2020). and the peaks around 1032 cm^{-1} are due to C-N stretching

of amines (Sharma et al., 2021). The FT-IR analysis of the methanol extract revealed the presence of bioactive compounds such as flavonoids, polyphenols, and alkaloids with substantial number of oxygen, nitrogen containing functional groups as well as aromatic ring. These compounds possess active binding sites that enable them to adsorb onto the surface of a material, such as a metal surface, effectively blocking potential corrosion sites when exposed to aggressive environments (Ji et al., 2015). This observation reflected the possible active groups which would be responsible for the adsorption process and will serves as a highly effective corrosion inhibitor.

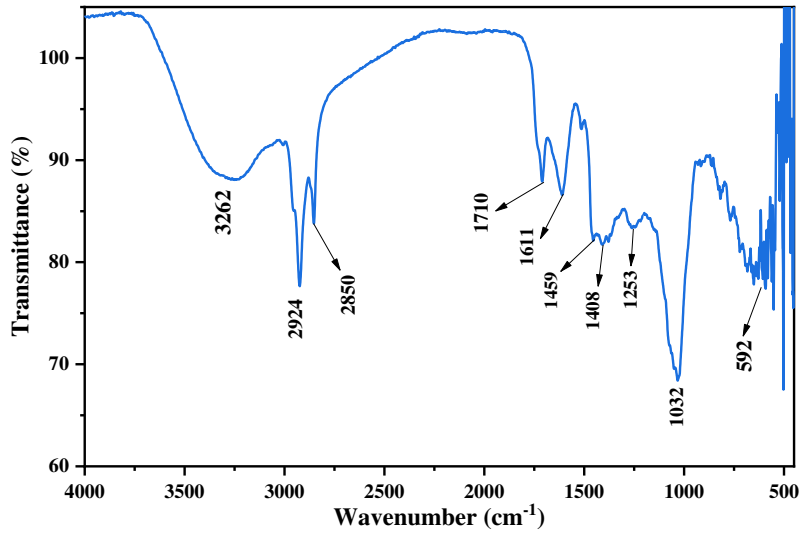

Figure 5: *FTIR spectrum of methanol extract*

4.3. Weight Loss Measurements

4.3.1. Effect of immersion time

The impact of varying immersion durations (ranging from 0.5 hours to 24 hours) on corrosion inhibition was investigated through a series of weight loss experiments. Experiments were performed in different concentration of inhibitor at laboratory temperature (18 °C). The weight loss of MS coupons in gram per unit area has been determined and tabulated in the Table 2. It has been observed that the MS sample immersed in the acid-only solution experiences significantly greater weight loss compared to the sample immersed with the inhibitor solution. For an instance, the weight loss of sample immersed for half an hour in acid only is 0.0027 g/cm^2 whereas for 1000 ppm inhibitor solution is 0.0002 g/cm^2. Similarly, for 1 h immersed sample, it

is 0.004 g/cm^2 and 0.0012 g/cm^2 respectively for acid only and 1000 ppm inhibitor solution. The trend is same for all immersion time, as it is 0.0529 g/cm^2 and 0.0114 g/cm^2 for 24 h immersed sample. This confirmed that the inclusion of inhibitors in a corrosive environment leads to a reduction in the weight loss of mild steel (MS). The weight loss in MS immersed in an acid-only (control) is high than that immersed in the presence of inhibitor solutions. This could be due to protecting role of inhibitor (Parajuli et al., 2022).

Table 2: *Variation of weight loss of MS sample with varying immersion times at different concentrations of inhibitors*

	Weight loss (g/cm^2)					
Time (h)	Control	200 ppm	400 ppm	600 ppm	800 ppm	1000 ppm
0.5	0.0027	0.0019	0.0012	0.0009	0.0003	0.0002
1	0.004	0.0028	0.00227	0.0019	0.0013	0.0012
3	0.008	0.0045	0.0029	0.0031	0.0027	0.0027
6	0.0242	0.0185	0.0119	0.0099	0.008	0.0065
9	0.1353	0.1099	0.0706	0.0508	0.0472	0.0281
18	0.0479	0.0251	0.0191	0.012	0.0119	0.0108
24	0.0529	0.0281	0.0248	0.0227	0.0115	0.0114

From the observation of above table, the slight increase in weight loss, even in the presence of inhibitors, may be attributed to desorption phenomena. Which may occur due to factors such as molecular size, orientation, and exposure time (Thapa et al., 2022). On exposing MS sample for a longer time, desorption of molecule from MS surface takes place and hence causes weight loss. Understanding and addressing these desorption mechanisms is crucial for the development of more effective corrosion inhibition strategies.

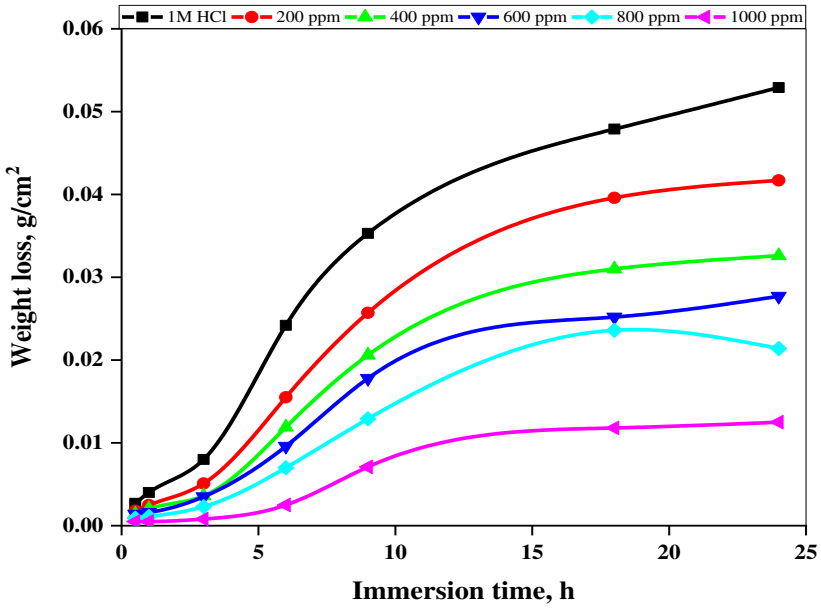

Figure 6: *Variation of weight loss with immersion time for MS sample immersed in the different inhibitor concentrations at room temperature*

It is found that inhibition efficiency gradually increased up to 3 h immersion time; however, with further extended immersion periods, there is a decline in efficiency. This decrease in efficiency is due to the dynamic desorption/absorption of inhibitor constituents at the metal/solution interface. The inhibition efficiency of 3-hour immersion is found to be maximum (90.34%) for the MS immersed in 1000 ppm inhibitor solution. The corrosion inhibition efficiency of the inhibitor molecules of various concentrations in 1 M HCl for MS samples immersed for different immersion time is shown in Figure 7.

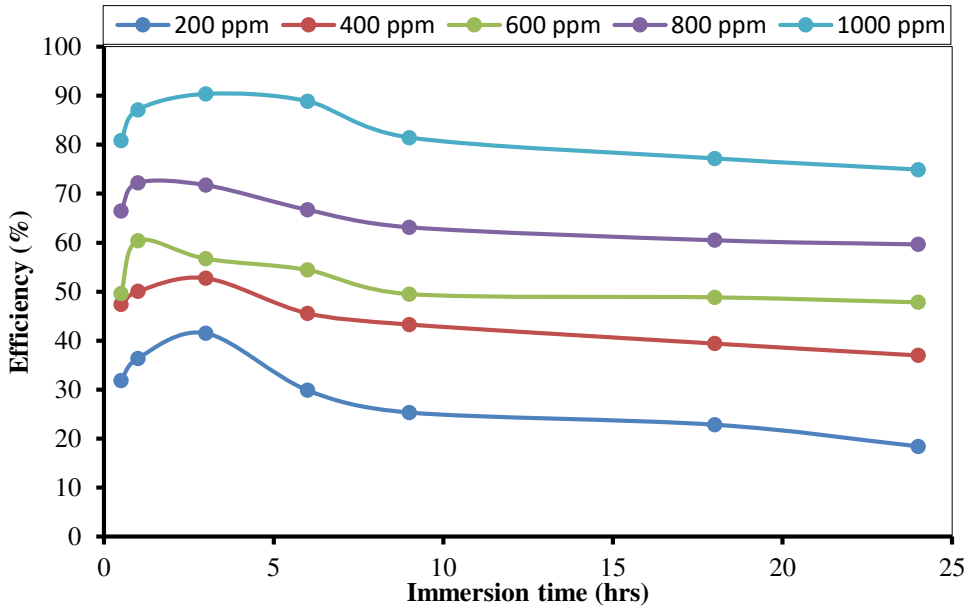

Figure 7: *The inhibition efficiency of inhibitor in 1 M HCl solution for the corrosion of mild steel immersed at a different time interval*

4.3.2. Effect of inhibitor concentration

The effectiveness of the inhibitor solution to resist corrosion is dependent on its concentration. In this experiment, the corrosion of MS surface immersed in solutions containing inhibitors at diverse concentrations (200, 400, 600, 800, and 1000 ppm) were examined. The experimental results, illustrated in Figure 8, demonstrated that, an incremental rise in inhibitor concentration corresponded to a gradual reduction in the weight loss experienced by mild steel (MS) specimens. For instance, The weight loss of the MS specimen after a 24-hour immersion in a 200 ppm solution measured at 0.0417 g/cm², whereas in 1000 ppm for same time is 0.0125 g/cm^2. Likewise, the weight loss of sample immersed for 9 h is 0.0257 and 0.0071 g/cm^2 respectively for 200 and 1000 ppm inhibitor solution. Similar is the trend for all immersion time. This implies that on increasing inhibitor concentration, there is decrease in weight loss of the sample. This could be due to the increased number inhibitor molecules which are responsible for covering of sample surface (Shrestha et al., 2019).

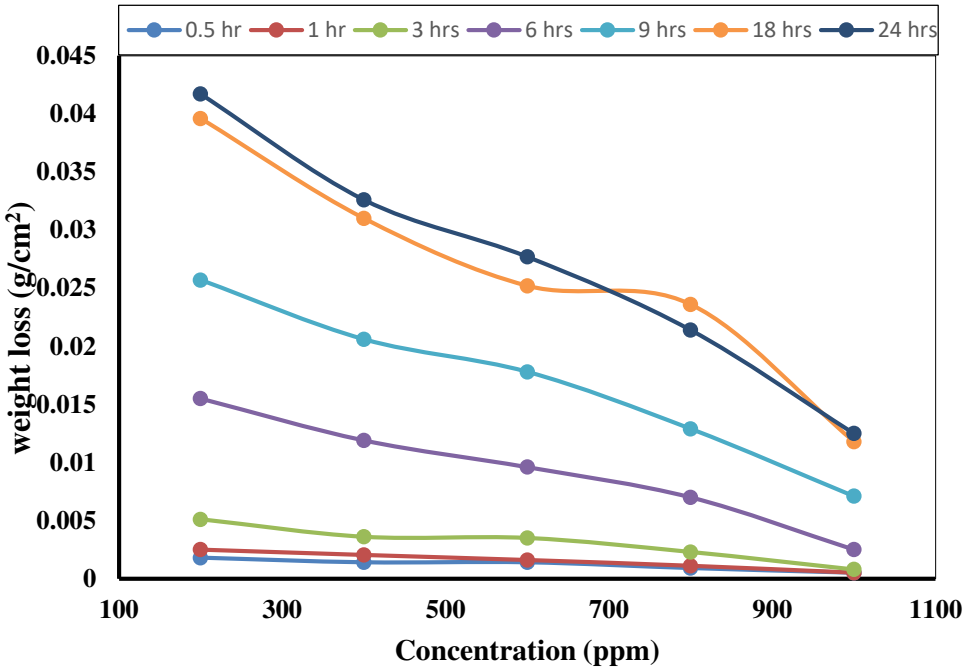

Figure 8: *Variation of weight loss versus concentration of extract on mild steel in 1 M HCl solution at various times*

Corrosion inhibition efficiency of MS immersed in 1 M HCl as a function of inhibitor concentration at different immersion time are shown in figure 9. It is clear that the rate of mild steel dissolution was lowered, while inhibition efficiency increased with increase in inhibitor concentration. The reason behind this fact can be given as adsorption of the organic matters of the extracts on metal surface. The maximum inhibition efficiency of 1000 ppm inhibitor solution is found to be 90.34% at 3 hours of immersion time. However, this efficiency did not remain stable as the immersion time continued to increase. Over an extended immersion period of 24 hours, the inhibition efficiency decreased to a minimum of 74.90% for the 1000 ppm inhibitor concentration. These findings highlight the time-dependent behaviour of the inhibitor and its varying effectiveness in preventing corrosion at different immersion durations.

Table 3: *Inhibition efficiency (%) of different concentrations of inhibitor at different immersion times*

	Inhibition efficiency (%)						
Conc.(ppm)	0.5 hr	1 hr	3 hr	6 hr	9 hr	18 hr	24 hr
200	31.83	36.39	41.52	29.87	25.32	22.83	18.42
400	47.39	50.05	52.76	45.59	43.31	39.43	37.01
600	49.59	60.42	56.73	54.45	49.52	48.85	47.83
800	66.47	72.22	71.76	66.73	63.16	60.52	59.67
1000	80.81	87.12	90.34	88.87	81.45	77.19	74.90

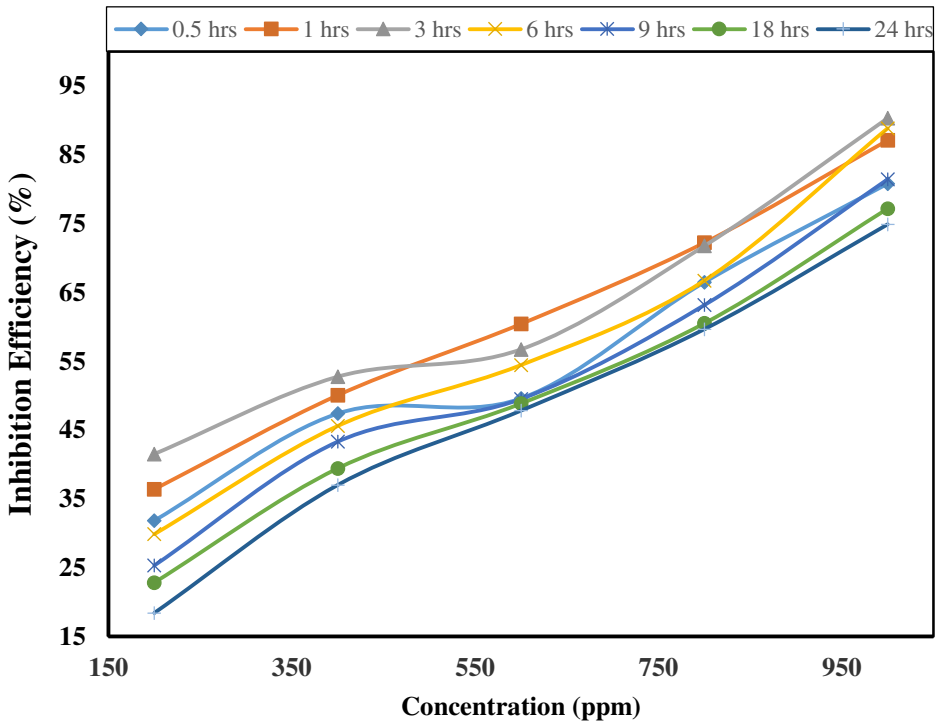

Figure 9: *Inhibition efficiency at different concentrations of inhibitor on mild steel in 1 M HCl solution at various immersion times*

4.3.3. Effect of working temperature

The weight loss measurement of different inhibitor solutions in different temperatures was measured. During the measurement, the MS coupons were immersed in these inhibitor solutions at different temperatures (18, 28, 38, 48, and 58 °C) for one hour. Observed data are tabulated in table 4.

Table 4: *Weight loss of MS immersed in different concentrations of inhibitor at different temperatures*

	Weight loss (g/cm^2)				
Concentration	18 °C	28 °C	38 °C	48 °C	58 °C
Control	0.0040	0.0137	0.0391	0.1790	0.5664
200 ppm	0.0025	0.0100	0.0300	0.1673	0.5476
400 ppm	0.0020	0.0070	0.0226	0.1349	0.4976
600 ppm	0.0016	0.0056	0.0190	0.1108	0.3831
800 ppm	0.0011	0.0043	0.0133	0.0772	0.2844
1000 ppm	0.0005	0.0021	0.0085	0.0554	0.2178

As the temperature increased, the weight loss of MS in inhibitor solutions is also increased. The maximum weight loss is found to be 0.5664 g/cm^2 at 58 °C in acid only solution. Which gradually decreases with increasing concentration of inhibitor. On increasing the temperature from 18°C to 58°C the weight loss is increased gradually. This increase in weight loss could be attributed to two potential reasons: desorption of inhibitor molecules from the MS surface and the structural deformation of the inhibitor molecules. Consequently, the increase in weight loss resulted in a decrease in the inhibition efficiency of the inhibitor.

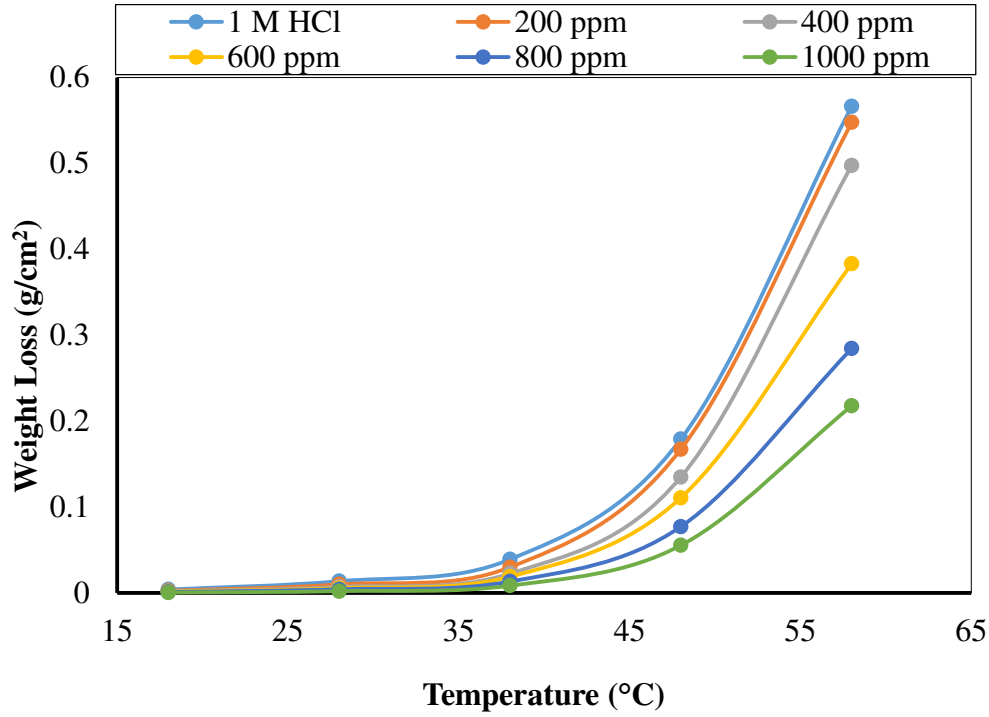

Figure 10: *Variation of weight loss of MS coupons in different concentration of inhibitor in 1 M HCl medium at different temperatures*

The effect of temperature on corrosion inhibition with different concentration of inhibitor was investigated by conducting experiments at various temperatures at a constant immersion time (1 h). The data obtained from these experiments were presented in Table 5. From this table, it is evident that the highest inhibition efficiency was observed at 18 °C. As the temperature rises above 28 °C, the inhibition efficiency becomes almost negligible at 200 ppm. But, at higher inhibitor concentrations, inhibition is still achieved even at elevated temperatures because the structural deformation of molecules may occur to a greater extent than desorption of molecules

from the material's surface. This deformation leads to the drastically decrease in inhibition efficiency of inhibitors for MS in the acidic medium above 58 °C.

Table 5: *Inhibition efficiency (%) of the inhibitor of different concentration on MS at different temperatures*

	Inhibition efficiency (%)				
Conc. (ppm)	18 °C	28 °C	38 °C	48 °C	58 °C
200	36.39	27.64	22.99	9.89	4.61
400	50.05	48.55	41.92	23.81	12.76
600	60.42	59.43	51.40	38.18	34.93
800	72.23	69.47	67.53	57.06	49.90
1000	87.12	84.59	78.13	68.92	61.01

The temperature dependence inhibition efficiency was studied and shown in the figure below. The maximum inhibition efficiency of 87.12% in 1000 ppm inhibitor solution at 18 °C temperature was achieved.

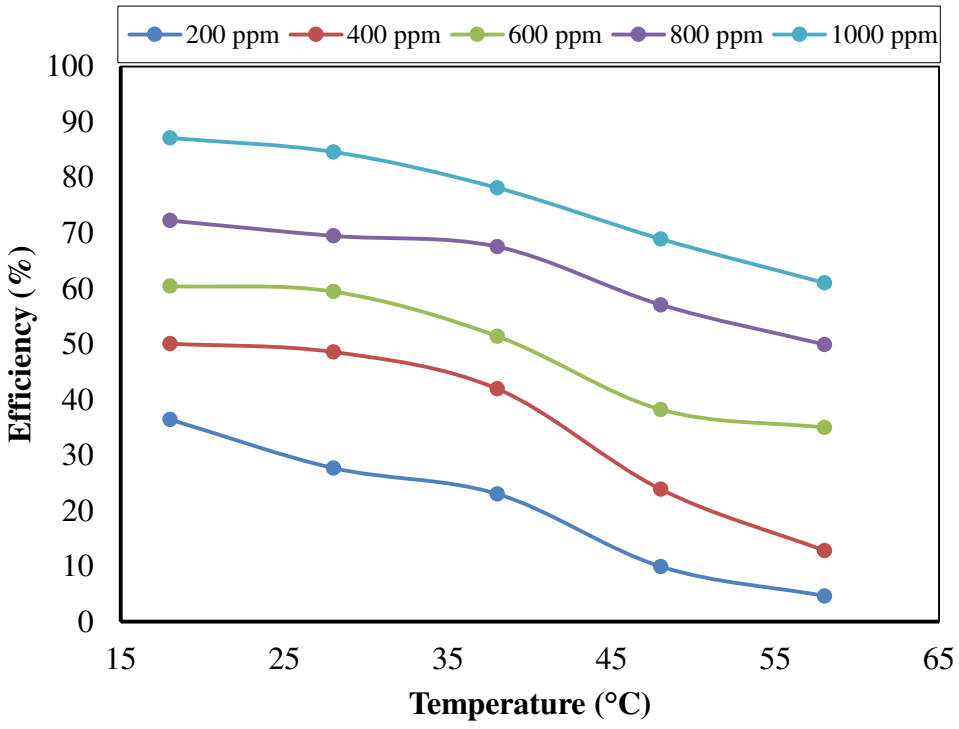

Figure 11: *Effect of temperature on the Inhibition efficiency of the alkaloids in 1 M HCl for MS corrosion*

4.4. Adsorption Isotherm

Adsorption isotherms provide information about the relationship between the concentration of a corrosion inhibitor and the amount of inhibitor adsorbed on the metal surface at a specific temperature. To study the adsorption isotherm, MS coupons are immersed in inhibitor solutions of different concentrations at laboratory temperature. When MS is immersed in an inhibitor solution, bulky organic molecules of inhibitors are adsorbed on the MS surface resulting in a decrease in the corrosion of MS. These adsorbed phytochemical block the active sites between the metal surface and acid molecules by restricting both anodic and cathodic reaction progress.

Adsorption isotherm provides basic information on how the inhibitor interacts with the MS surface. In the aqueous inhibitor solution, the adsorption of inhibitor molecule on MS surface always takes place after replacing the adsorbed water dipole. And the phenomenon is a quasi-substitution process (Fouda et al., 2021).

In order to identify the adsorption phenomenon, the interactive nature of molecules, the free energy of adsorption, and the thickness of the adsorptive layer. Different adsorption isotherms are studied.

4.4.1. Langmuir adsorption isotherm

Langmuir's adsorption isotherm equation can provide insights into whether the adsorption process is monolayer or multilayer. Langmuir isotherm has been tested by plotting C/θ versus C (mol/L). Concentration of inhibitor in (mol/L) is obtained by dividing ppm concentration by Molecular weight of Chrysin × 1000. For θ value, the data of 3 h immersion is used. If the slope of the curve, obtained by plotting C/θ against C, is equal to one, it signifies that monolayer adsorption is taking place(Ayoola et al., 2022).

$$\frac{C}{\theta} = \frac{1}{K} + C \qquad \ldots(8)$$

As we plot $\frac{C}{\theta}$ vs C, a straight line with R^2 value equal 0.9274 is obtained as in table 6. This value is highly deviated from unity, showing that the adsorption of inhibitor molecules on MS surface does not follow the assumptions of the Langmuir model. This indicates that adsorption may be mono- or multilayer but the complete monolayer has not been formed before multilayer formation. The value of slope and R^2 strongly deviated from unity indicated that the adsorption process in this corrosion inhibition

mechanism cannot be adequately explained by the Langmuir isotherm model. (Neha et al., 2015).

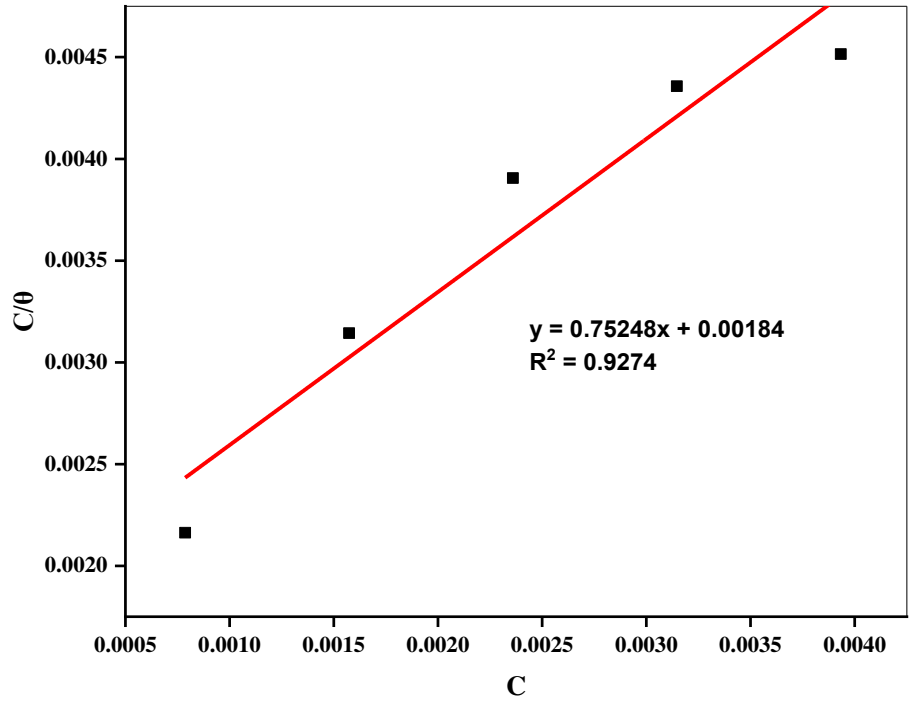

Figure 12: *Langmuir adsorption isotherm plot for MS in 1 M HCl with different concentration of inhibitor*

4.4.2. Freundlich adsorption isotherm

The linear form of Freundlich model can also be employed to determine the ease of adsorption of inhibitor molecules on the metal surface. Using the following formula, the Freundlich adsorption isotherm can be calculated,

$$\ln \theta = \frac{1}{n} \ln C + \ln K \qquad \ldots(9)$$

A graph of straight line (R^2 value 0.9865) obtained by plotting ln θ versus ln C, with slope value (1/n) equal to 0.5264, which is lies between 0 and 1 i.e., 0<1<n<1. It indicates that the adsorption process is relatively easy (Ituen et al., 2017).

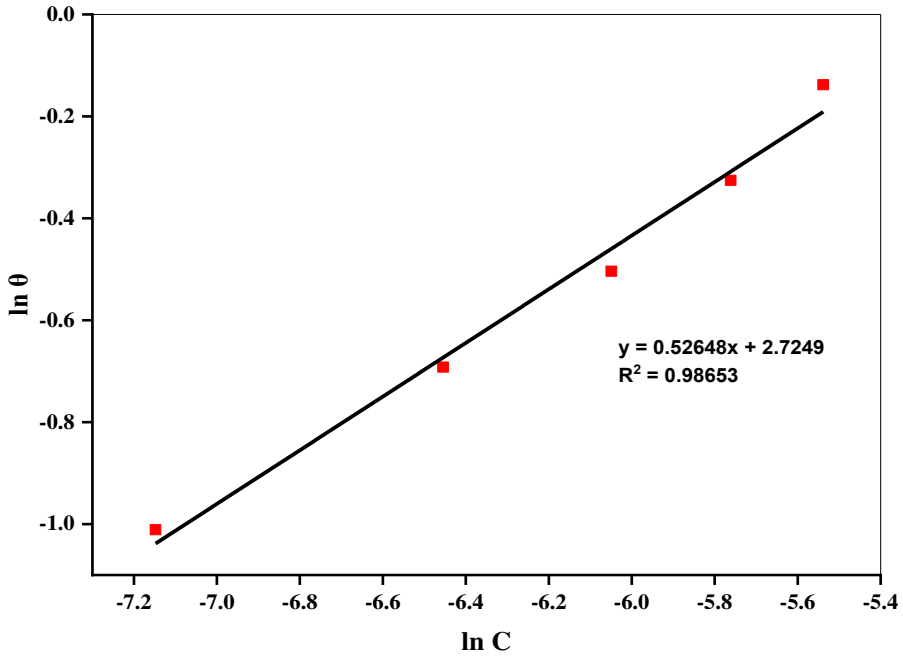

Figure 13: *Freundlich adsorption isotherm for MS in 1 M HCl medium.*

4.4.3. Temkin adsorption isotherm

Temkin adsorption isotherm was evaluated for the explanation of corrosion inhibition mechanism and the nature of interaction taking place in the adsorbed layer (Ituen et al., 2017). The slope and R^2 value of linear form of Temkin adsorption isotherm was found to be 0.2984 and 0.9384 respectively. This is obtained by plotting Θ vs lnC in equation (10).

$$\theta = -\frac{1}{2a} ln\, C - \frac{1}{2a} ln\, K \qquad \ldots(10)$$

The molecular interaction parameter (a), which is calculated from the slope of the straight line in figure 14, is found to be negative 1.675, suggesting that there is strong interaction between the inhibitor molecules. From intercept of curve, the value of '*K'* is found to be negative 2.1092, indicating inhibitor molecules are strongly absorbed on the MS surface (Thapa et al., 2022).

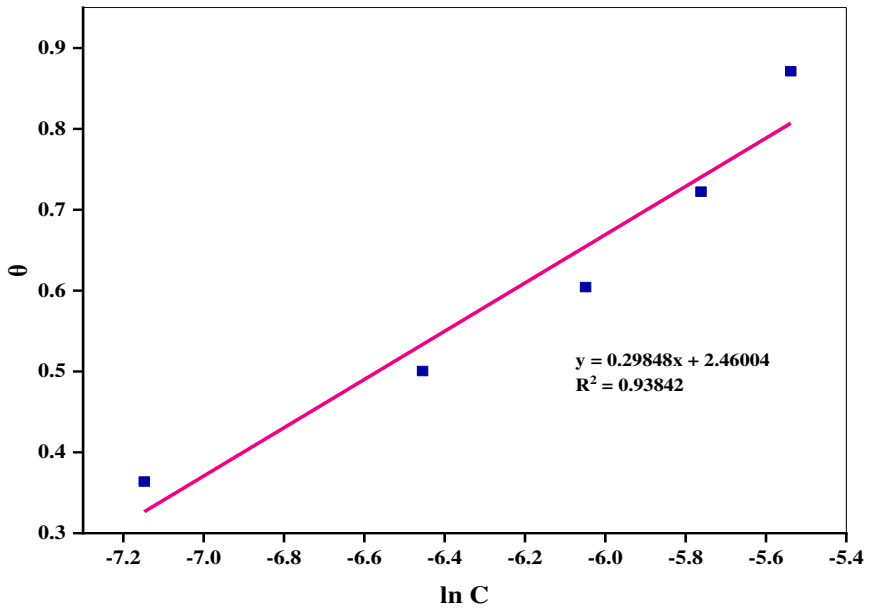

Figure 14: *Temkin adsorption isotherm plot for MS in 1 M HCl with different concentration of inhibitor*

The values of slope and intercept have their usual significances which have been explained above. In order to assess whether the measured values are acceptable, the linearity range can be checked using the R^2 value, which provides the correlation between the measured values. Three different R^2 values are listed in table 6 for three different isotherms. Among them, the R^2 value for Langmuir isotherm is highly deviated whereas for Temkin it is more nearer to unity and for Freundlich isotherm, it is quite acceptable and equal to 0.9865 and it describes heterogeneous adsorption systems. Since the given data are not fitted properly for Langmuir isotherm model so that the value of Gibb's free energy has not been calculated here.

Table 6: *Different adsorption isotherm model and their parameters*

Isotherm	Plotting	Slope	Intercept	R^2
Langmuir	C/θ vs C	0.7524	0.0018	0.9274
Freundlich	ln θ vs ln C	0.5264	2.7249	0.98653
Temkin	θ vs ln C	0.2984	2.4600	0.93842

4.5. Activation Energy and Corrosion Kinetics

By rearranging the Arrhenius equation and and replacing rate of reaction by corrosion rate, the activation energy of the reaction between inhibitor solution on MS surface can be determined and it is directly related to the corrosion rate (Ostovari et al., 2009).

$$\log(CR) = \log A - \frac{E_a}{2.303RT} \qquad \ldots(11)$$

Where A is the Arrhenius pre-exponential constant, T is the absolute temperature. The activation energy of the reaction is equal to the slope of the Arrhenius plot obtained by ploting log(CR) vs $\frac{1}{2.303RT}$.

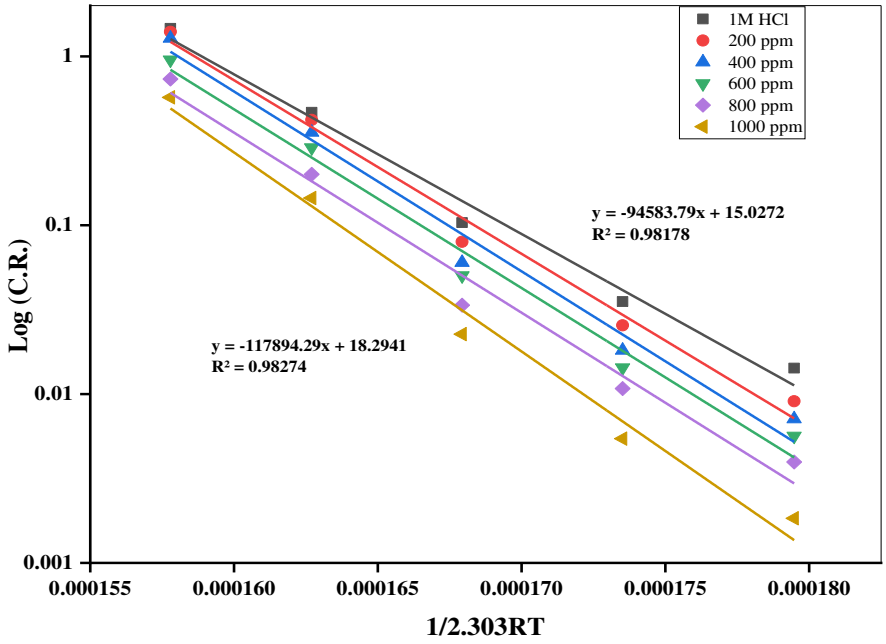

Figure 15: *Arrhenius plot for MS in 1 M HCl with and without inhibitor*

Energy of activation for those system was evaluated from slope of the curve. It is found that the activation energy for acid only system is 94583.79 J/mol whereas for 1000 ppm inhibitor solution it is 117894.29 J/mol. It reveals that the activation energy of the reaction increased in the presence of inhibitor, This implies that the inhibitor molecules helped to retard the corrosion rate by increasing activation energy (Karki et al., 2021). The trend for increasing activation energy has not been changed implying that the reaction pathway has been altered by same mechanism by all concentration of inhibitors.

4.6. Thermodynamics of Corrosion

Enthalpy and entropy of the system can be determine by using the transition state equation which is an alternative form of the Arrhenius equation, (Akinbulumo et al., 2020).

$$\log\left(\frac{CR}{T}\right) = \log\frac{R}{hN} + \frac{\Delta S}{2.303R} - \frac{\Delta H}{2.303RT} \qquad \ldots(12)$$

Where, 'N' is Avogadro's number, 6.0225×10^{23} mol^{-1} and 'h' is plank's constant, 6.6261×10^{-34} Js, (ΔH^{o}) is the enthalpy of activation which is obtained as slope of equation (12) by plotting $\log\left(\frac{CR}{T}\right)$ vs. $\frac{1}{2.303RT}$ and (ΔS^{o}) is entropy of activation which can be calculated from its intercept.

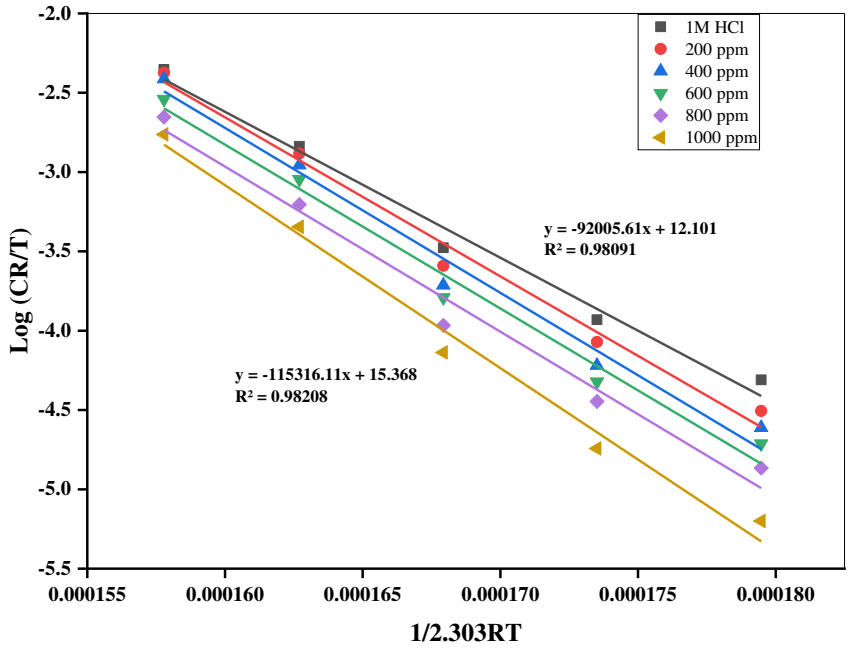

Figure 16: *Transition state plot for MS in 1 M HCl with and without inhibitor*

Based on the observation, it was found that the enthalpy (ΔH°) of the system in the presence of an inhibitor appeared higher than in the absence of an inhibitor. The adsorption process being endothermic is indicated by the positive ΔH° value during the adsorption of the inhibitor on the MS surface (Karki et al., 2021). The value of enthalpy was increased gradually with an increase in concentration of inhibitor solution from 92.005 kJ mol^{-1} to 115.31 kJ mol^{-1}, indicates a corrosion rate controlled by kinetic parameters of activation. Likewise the energy of activation (E_a) of the system was also

increased with the addition of inhibitors of higher concentrations leading to a reduction in the reaction rate (Ituen et al., 2017)

Similarly, from the intercept of the transition state plot, the entropy of the system (ΔS°) is determined. The value entropy increased from 34.125 kJ mol^{-1} of acid only solution to 96.678kJ mol^{-1} in 1000 ppm inhibitor solution. This increase in entropy or randomness in the transition state is primarily caused by the formation of activated complexes, indicating associative mechanisms (Thapa Magar et al., 2023). Thus obtained values of E_a, ΔH°, and ΔS° are tabulated in Table 7.

Table 7: *Thermodynamic parameters of the MS in different concentration of inhibitor medium*

Electrolyte	Log (A)	Ea(KJ/mol)	ΔH˚ (KJ/mol)	Ea-ΔH˚	ΔS˚(J/mol/K)
Acid	15.02	94.58	92.005	2.57	34.1256
200 ppm	16.31	102.83	100.25	2.57	58.7406
400 ppm	16.84	106.55	103.97	2.57	68.8560
600 ppm	16.62	105.87	103.30	2.57	64.7606
800 ppm	16.61	106.66	104.08	2.57	64.5296
1000 ppm	18.29	117.89	115.31	2.57	96.6782

From the above table, the value of energy of activation (E_a) is higher than enthalpy (ΔH°), indicating a cathodic hydrogen evolution reaction leading to a decrease in total reaction volume. The difference between E_a and ΔH° is found to be 2.58 kJ mol^{-1}, this is very close to the value of RT, indicating that the adsorption of inhibitor on MS surface primarily follows physical dominant chemical adsorption (Ituen et al., 2017).

4.7. Electrochemical Methods

4.7.1. Polarization measurement of as-immersed MS sample

For as immersed condition, potentiodynamic polarization experiment was carried out by immersing the MS in different inhibitor concentrations (200, 400, 600, 800, and 1000 ppm), and a potential of 300 millivolts was applied in both the cathodic and anodic direction. In the acid-only solution, the current density was measured to be 27.5 μA/cm². However, with the addition of different concentrations of inhibitors, the corrosion current density gradually decreased. Specifically, it decreased to 0.018 mA/cm² when using a 1000 ppm inhibitor solution. This decrease in current density in presence of inhibitor implies that inhibitor molecules restrict the follow of electron in the cell system and thereby reduce carrion current density. This restriction in the follow of electron could be either by asymmetric effect or by adsorption of inhibitor molecules

on the mild steel surface (Thapa et al., 2022). The polarization measurement data obtained from tafel plot are tabulated in table 8.

Table 8: *Variation of inhibitor concentration on current density, and inhibition efficiency for for as-immersed condition*

Medium	Ecorr (V)	Icorr (μA/cm^2)	Anodic slope (V/decade)	Cathodic slope (V/decade)	Efficiency (%)
Acid	-0.467	27.5	0.0775	0.1457	
200	-0.469	26.1	0.0667	0.1143	5.09
400	-0.464	14.7	0.0806	0.139	46.55
600	-0.481	10	0.0787	0.1193	63.64
800	-0.491	11.7	0.0923	0.187	57.45
1000	-0.494	9.32	0.0703	0.1116	66.11

The polarization curves (Figure 17) indicate that the current density decreases slightly for lower inhibitor concentrations (200 ppm and 400 ppm) but decreases noticeably for higher inhibitor concentrations (600 ppm, 800 ppm, and 1000 ppm). Overall, the trend observed in the data supports the notion that higher concentrations of inhibitors lead to a more significant reduction in the corrosion rate of the as-immersed MS sample.

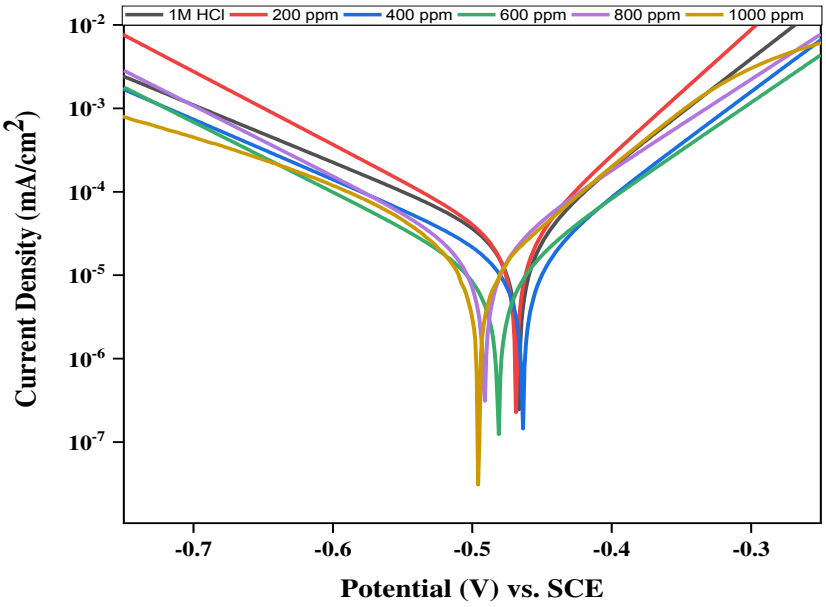

Figure 17: *Potentiodynamic polarization curve for mild steel immersing with 1 M HCl solution containing different concentrations of inhibitor for as-immersed conditions*

4.7.2. Polarization measurement of 1h-immersed MS sample

Potentiodynamic polarization measurements were carried out after immersing MS samples in different concentrations of inhibitor solutions for 1 h in the potential window

of -0.8 to - 0.2 V. A plot of the logarithmic function of corrosion current density versus potential is plotted as shown in Figures 18. The current density in acid only solution is 24.8 μA/cm^2 whereas in 200 ppm solution is 7.37 μA/cm^2 which gradually decreases and reached to 5.66 μA/cm^2 in 1000 ppm solution. Thus on increasing the concentration of inhibitor solution, corrosion current density is decreased. This implies that the quantity of inhibitor molecules adsorb on MS surface also increases. These increasing number of molecules either show asymmetric effect or get adsorbed on the steel surface. For both of the cases, increased number of molecules get much more pronounced resulting the decrease in current density. The adsorbed molecules also cover more fraction of steel surface and form a protective layer (Karki et al., 2021).

The potentiodynamic polarization measurement of corrosion current densities and inhibition efficiency of various inhibitor solution immersed on MS surface for 1 hr immersion condition with their corresponding anodic, cathodic slope, are tabulated in table 9.

Table 9: *Variation of inhibitor concentration on current density, and inhibition efficiency for 1hr immersed condition*

Medium	Ecorr (V)	Icorr (μA/cm^2)	Anodic slope (V/decade)	Cathodic slope (V/decade)	Efficiency(%)
Acid	-0.486	24.8	0.0947	0.118	
200	-0.497	7.37	0.1486	0.1568	70.28
400	-0.491	6.81	0.1369	0.1585	72.54
600	-0.492	6.64	0.1118	0.1379	73.23
800	-0.485	6.11	0.0935	0.1053	75.36
1000	-0.506	5.66	0.0784	0.1105	77.18

Since the anodic and cathodic slopes of the polarization curves are not changed. They are in same trend with acid only solution which indicates that the inhibitor molecules are not changing the reaction pathway for inhibition. Also, there is fluctuation in the corrosion potential. It is -0.486V for acid and maximum -0.506 V for 1000 ppm inhibitor. This deviation is equal to 20 mV which is less than 85 mV. This also indicates that the inhibitor tested here works as mixed type of inhibitor.

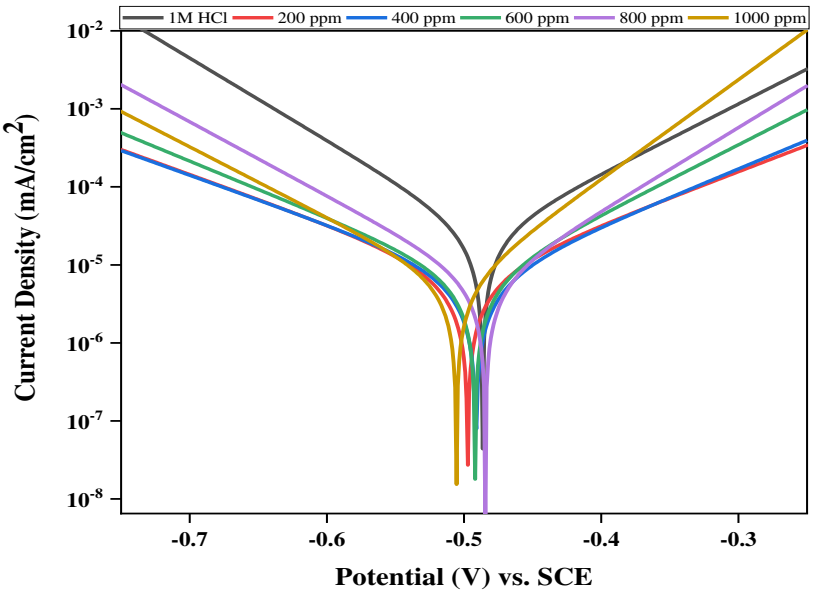

Figure 18: *Potentiodynamic polarization curve for mild steel immersing with 1 M HCl solution containing different concentrations of inhibitor for 1 h immersed condition*

The inhibition efficiency for 200 ppm is 70.28% which gradually increases up on addition of more concentration of inhibitor and reaches to 77.18% for 1000 ppm solution. The inhibition efficiency just increased by 6.9% up on increasing the concentration of inhibitor by 800 ppm. One can conclude that this could be due to saturation of inhibitor concentration however this is not true. The inhibition efficiency does not only depend on the concentration but also the orientation of the adsorption, size of inhibitor molecule and also size of the inert hydrocarbon groups of inhibitor (Karki et al., 2021).

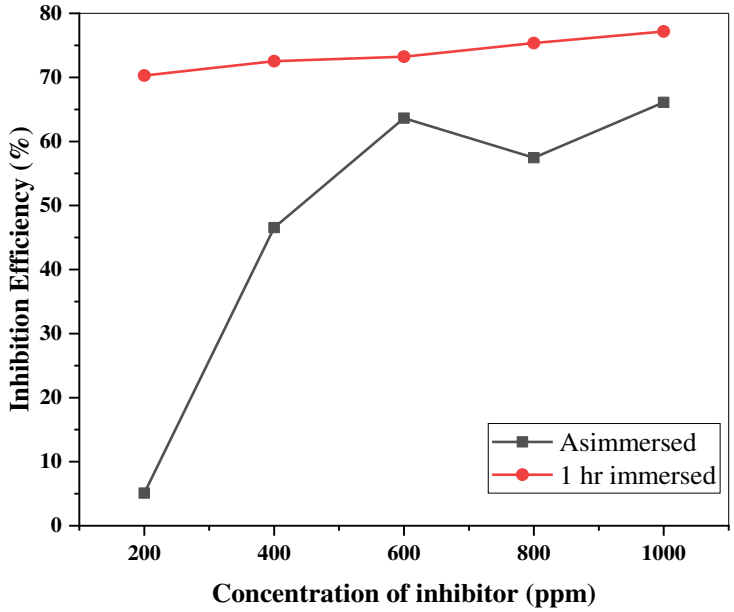

Figure 19: *variation of Inhibition efficiency with different concentration of inhibitor for both as-immersed and 1 h immersed condition*

4.7.4. Electrochemical Impedance Spectroscopy (EIS)

EIS measurement was performed by the analysis of Nyquist and Bode plots. The capacitive loop diameter of the semicircle in the Nyquist plot represents the charge transfer resistance (R_{ct}) and it is increased with the increase in concentration of inhibitor solution. Charge transfer resistance is obtained as the difference between real axis impedance at the initial and final frequencies. From the values of the charge transfer resistance of the inhibited ($R_{ct\ (inh)}$) and the blank solution (R_{ct}), the inhibition efficiency (% IE) is calculated using the equation (6).

Nyquist plot in figure 20 showed that, by increasing the inhibitor concentration up to 1000 ppm the impedance (R_{ct}) values rises to 2100 Ω. Which is due to the consequence of adsorption inhibitor molecules on the metal surface by displacing water dipoles. which decelerates the rate of metal dissolution (Karki et al., 2021).

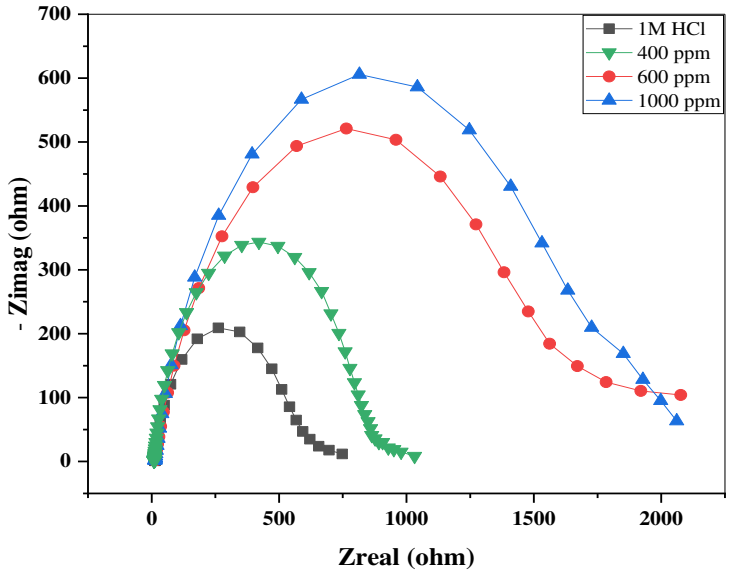

Figure 20: *Nyquist plots of different concentrations of inhibitor in 1 M HCl for 1 h immersed condition on MS surface*

The impedance parameters derived from EIS measurement are presented Table 10. The fitted parameters calculated using equivalent circuit using Z view software. From above table, it is clear that by increasing the concentration of the inhibitor the polarization resistance (R_{ct}) increases due to which the inhibition efficiency also increases. The maximum inhibitory performance of 71.86% was observed for MS in the 1000 ppm solution, while the lowest inhibition efficiency of 30.50% was noted for the 400 ppm inhibitor solution. This variation is due to the formation of the thin protecting layer of inhibitor on the MS interface and acts as barrier for corrosive ions by increasing the interfacial resistance of the MS surface (Khaled & Abdel-Rehim, 2011).

Table 10: *Parameters EIS for corrosion of MS in 1M HCl with different concentration of inhibitor*

Concentration (ppm)	*R_{ct} (Ωcm^2)*	*IE%*
1M HCl	590	
400 ppm	850	30.50
600 ppm	1683	64.90
1000 ppm	2100	71.86

In Bode Magnitude plot, it was observed that the impedance at higher frequencies was approximately 16 Ω, indicating a highly conductive nature of the solution. However, in the lower frequency range, the impedance of acid only solution is 660 Ω whereas impedance of 1000 ppm inhibitor solution is 2374Ω as in figure 21. Here, an increase in the magnitude of impedance (|Z|) in the low-frequency region on increasing inhibitor concentration represented a decrease in electron flow through the MS surface and thus minimize the corrosion reaction (Laschuk et al., 2021).

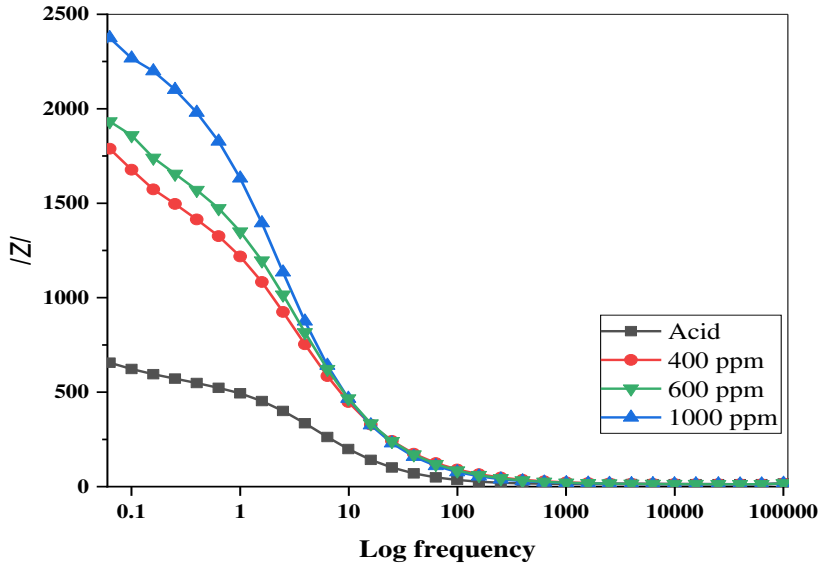

Figure 21: *Bode magnitude plot obtained from EIS measurement of MS sample in 1 hour immersed condition*

Figure 22 demonstrates that the phase angle in the Bode-phase plot rises as the inhibitor concentration increases up to 1000 ppm, providing further confirmation of adsorption inhibitor molecules on MS surface also rises by reducing active sites for reaction with acid molecules (Khaled & Abdel-Rehim, 2011).

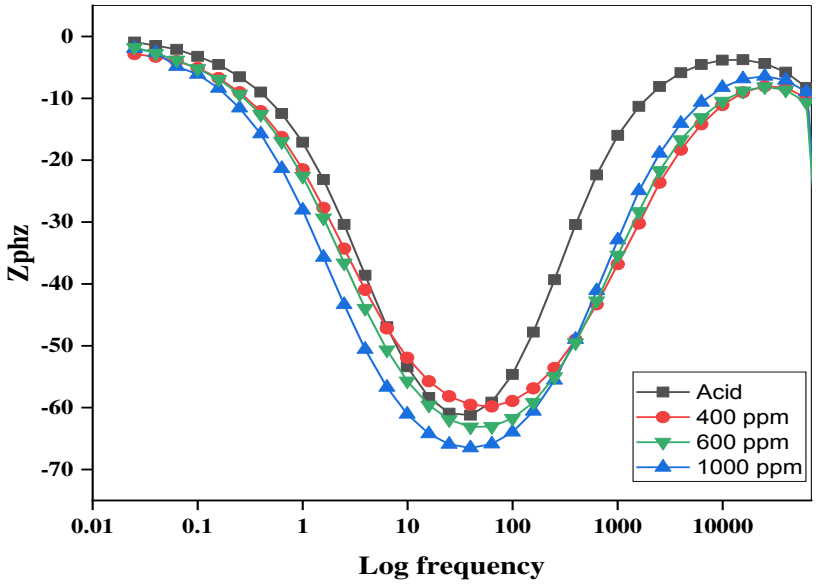

Figure 22: *Bode plots of phase angle vs. frequency for mild steel in 1 M HCl containing different concentrations of inhibitor immersed for 1 h condition*

4.8. Mechanism of Corrosion Inhibition

The plant extract has several phytochemicals present in it. Therefore, with the help of these phytochemicals plant extract get absorbed into the metal substrate surface and follow chemisorption, physisorption, and Reterodonation (Bhardwaj et al., 2021). Physisorption of an inhibitor occurs when the inhibitor molecules weakly attract to the metal surface, primarily through van der Waals forces. In contrast, chemisorption involves a stronger interaction between the surface and adsorbate inhibitor molecules, forming hydrogen, covalent, and ionic bonds. Reterodonation refers to the bonding that takes place between the electrons of the unsaturated part of a molecule and the surface of the substrate (Kairi & Kassim, 2013).

The adsorption of inhibitor molecules occurs through the replacement of water dipoles from the metal surface, as follows:

$$Org_{(sol)} + xH_2O_{(ads)} \longrightarrow Org_{(ads)} + H_2O_{(sol)}$$

Where, $Org_{(sol)}$ and $Org_{(ads)}$ denote the solvated and adsorbed organic molecules respectively. Likewise, $H_2O_{(ads)}$ represents water molecules adsorbed on the surface of mild steel (MS), and 'x' signifies the size ratio, which quantifies the number of water molecules substituted by a single organic molecule (Sadeghi Erami et al., 2019)

The activation energy in the acid only solution is measured at 94.58 kJ/mol, it increased gradually in the presence of different inhibitor concentration such as 102.83 kJ/mol in 200 ppm, 106.55 kJ/mol in 400 ppm, 105.87 kJ/mol in 600 ppm, 106.66 kJ/mol in 800 ppm and 117.89 kJ/mol in 1000 ppm, that consequently reduced rate of corrosion. Also, similar trend in the slope of the polarization curve indicates that there hasn't been any alteration in the reaction pathway. Thus the inhibitor molecules adsorbed on the MS surface form a protective layer by blocking both cathodic and anodic reactions simultaneously.

The hetero-elements such as oxygen (O), nitrogen (N), and sulphur (S) present in the phytochemicals when dissolved in acidic solution gets protonated. The acidic solution provides an excess of protons that can react with the available heteroatoms in the phytochemicals, leading to the formation of positively charged species which interact with chloride ions through the electrostatic force of attraction. The protonated phytochemicals, such as alkaloids, flavonoids, or terpenoids return to their neutral state after liberating H_2 molecules (Bhardwaj et al., 2021).

Then, the electron pair from the highest occupied molecular orbital (HOMO) of phytochemicals, particularly the lone pair on heteroatoms like nitrogen or oxygen, can form a coordinate covalent bond with the vacant d-orbital of an iron atom, leading to an accumulation of additional negative charge on the metal surface. In order to neutralize this charge, electrons are sent back to LUMO especially to anti-bonding π^* orbital of the organic molecule with a high orbital density. This retrodonation can further stabilize the complex and enhance the binding affinity between the inhibitor and the metal active site (Karki et al., 2021).

The Schematic diagram for the adsorption of phytochemical extract on MS surface is shown in Figure 23:

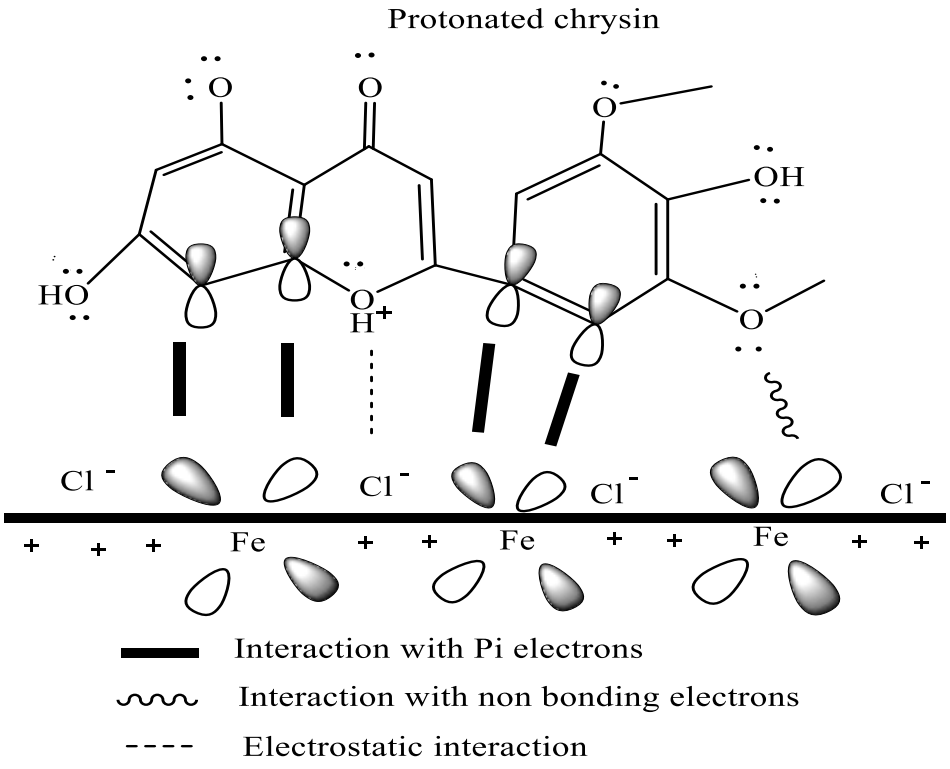

Figure 23: *Schematic diagram for different mode of adsorption of Inhibitor (Chrysin) molecules on mild steel/1 M HCl interface*

CHAPTER 5

CONCLUSION

In the present study, the methanol extract of *Colebrookea oppositifolia* was prepared as an effective inhibitor for mild steel in 1 M HCl solution and characterized by chemical and spectroscopic methods. The anti-corrosion behaviour and inhibition efficiency of the inhibitor was studied by weight-loss, potentiodynamic polarization (PDP), and electrochemical impedance spectroscopy (EIS) methods. A comparative study of corrosion at different periods and concentrations was done. From the data and results obtained, the following statements can be inferred;

- The weight loss of mild steel decreased with an increase in the concentration of the inhibitor in 1M HCl. Thus, decrease the corrosion rate.
- As the concentration of the inhibitor in the corrosive medium was raised up to 1000 ppm, the maximum inhibition efficiency of 90.34% was observed for weight loss measurement.
- From the study of different adsorption isotherm, the inhibitor adsorb on the mild steel surface follows the Freundlich adsorption model.
- Potentiodynamic polarization measurements showed that corrosion current density significantly decreases with an increase in inhibitor concentration and act as a mixed type of inhibitor for corrosion of steel in acidic solution.
- The polarization experiment results indicate that the highest level of inhibition efficiency was observed at 66.11% for the samples immersed in a 1000 ppm concentration under as-immersed conditions, and it increased to 77.18% when the samples were immersed for one hour under the same 1000 ppm concentration.
- FTIR results confirmed the presence of N-H, O-H, C-H, and C=O groups, providing the inhibitive property. The calculated thermodynamic parameters revel that the adsorption process is endothermic and is physically dominated by chemical adsorption.

Thus, it is clear from the study that the methanol extract of *Colebrookea oppositifolia* has the potential to serve as a highly effective and environmentally friendly corrosion inhibitor for mild steel in 1 M HCl solution.

REFERENCES

Ahamad, I., Prasad, R., & Quraishi, M. (2010). Adsorption and inhibitive properties of some new Mannich bases of isatin derivatives on corrosion of mild steel in acidic media. *Corrosion Science*, *52*(4), 1472–1481.

Ahmed, M. H. O., Al-Amiery, A. A., Al-Majedy, Y. K., Kadhum, A. A. H., Mohamad, A. B., & Gaaz, T. S. (2018). Synthesis and characterization of a novel organic corrosion inhibitor for mild steel in 1 M hydrochloric acid. *Results in Physics*, *8*, 728–733. https://doi.org/10.1016/j.rinp.2017.12.039

Ajaib, M., Abid, S., Anjum, M., Noshad, Q., Siddiqui, M. F., & Iqbal, M. A. (2018). 17. Phytochemical, antibacterial and antifungal activities of leaves and bark of Colebrookea oppositifolia: An ethnomedicinal plant. *Pure and Applied Biology (PAB)*, *7*(1), 138–151.

Akinbulumo, O. A., Odejobi, O. J., & Odekanle, E. L. (2020). Thermodynamics and adsorption study of the corrosion inhibition of mild steel by *Euphorbia heterophylla* L. extract in 1.5 M HCl. *Results in Materials*, *5*, 100074. https://doi.org/10.1016/j.rinma.2020.100074

Ayoola, A. A., Babalola, R., Durodola, B. M., Alagbe, E. E., Agboola, O., & Adegbile, E. O. (2022). Corrosion inhibition of A36 mild steel in 0.5 M acid medium using waste citrus limonum peels. *Results in Engineering*, *15*, 100490. https://doi.org/10.1016/j.rineng.2022.100490

Bahlakeh, G., Ramezanzadeh, B., Dehghani, A., & Ramezanzadeh, M. (2019). Novel cost-effective and high-performance green inhibitor based on aqueous *Peganum harmala* seed extract for mild steel corrosion in HCl solution: Detailed experimental and electronic/atomic level computational explorations. *Journal of Molecular Liquids*, *283*, 174–195. https://doi.org/10.1016/j.molliq.2019.03.086

Bhardwaj, N., Sharma, P., & Kumar, V. (2021). Phytochemicals as steel corrosion inhibitor: An insight into mechanism. *Corrosion Reviews*, *39*(1), 27–41.

Chapagain, A., Acharya, D., Das, A. K., Chhetri, K., Oli, H. B., & Yadav, A. P. (2022). Alkaloid of *Rhynchostylis retusa* as green inhibitor for mild steel corrosion in 1 M H2SO4 Solution. *Electrochem*, *3*(2), Article 2. https://doi.org/10.3390/electrochem3020013

Chen, S., Zhao, H., Chen, S., Wen, P., Wang, H., & Li, W. (2020). Camphor leaves extract as a neoteric and environment friendly inhibitor for Q235 steel in HCl medium: Combining experimental and theoretical researches. *Journal of Molecular Liquids*, *312*, 113433. https://doi.org/10.1016/j.molliq.2020.113433

Finšgar, M., & Jackson, J. (2014). Application of corrosion inhibitors for steels in acidic media for the oil and gas industry: A review. *Corrosion Science*, *86*, 17–41. https://doi.org/10.1016/j.corsci.2014.04.044

Fouda, A. E.-A. S., El-Askalany, A. H., Molouk, A. F., Elsheikh, N. S., & Abousalem, A. S. (2021). Experimental and computational chemical studies on the corrosion inhibitive properties of carbonitrile compounds for carbon steel in aqueous solutions. *Scientific Reports*, *11*(1), 21672.

Gadow, H., & Motawea, M. (2017). Investigation of the corrosion inhibition of carbon steel in hydrochloric acid solution by using ginger roots extract. *RSC Advances*, *7*(40), 24576–24588.

Haldhar, R., Prasad, D., & Bhardwaj, N. (2020). Experimental and theoretical evaluation of acacia catechu extract as a natural, economical and effective corrosion inhibitor for mild steel in an acidic environment. *Journal of Bio-and Tribo-Corrosion*, *6*(3), 76.

Hou, B., Li, X., Ma, X., Du, C., Zhang, D., Zheng, M., Xu, W., Lu, D., & Ma, F. (2017). The cost of corrosion in China. *Npj Materials Degradation*, *1*(1), 4.

Hussin, M. H., Jain Kassim, M., Razali, N. N., Dahon, N. H., & Nasshorudin, D. (2016). The effect of Tinospora crispa extracts as a natural mild steel corrosion inhibitor in 1M HCl solution. *Arabian Journal of Chemistry*, *9*, S616–S624. https://doi.org/10.1016/j.arabjc.2011.07.002

Ishtiaq, S., Hanif, U., Shaheen, S., Bahadur, S., Liaqat, I., Awan, U. F., Shahid, M. G., Shuaib, M., Zaman, W., & Meo, M. (2020). Antioxidant potential and chemical characterization of bioactive compounds from a medicinal plant Colebrokea oppositifolia Sm. *Anais Da Academia Brasileira de Ciências*, *92*(2), e20190387. https://doi.org/10.1590/0001-3765202020190387

Ituen, E., Akaranta, O., & James, A. (2017). Evaluation of performance of corrosion inhibitors using adsorption isotherm models: An overview. *Chemical Science International Journal*, *18*(1), 1–34.

Ji, G., Anjum, S., Sundaram, S., & Prakash, R. (2015). Musa paradisica peel extract as green corrosion inhibitor for mild steel in HCl solution. *Corrosion Science*, *90*, 107–117. https://doi.org/10.1016/j.corsci.2014.10.002

Kairi, N. I., & Kassim, J. (2013). The effect of temperature on the corrosion inhibition of mild steel in 1 M HCl solution by Curcuma longa extract. *Int. J. Electrochem. Sci*, *8*, 7138–7155.

Kalaiselvi, P., Chellammal, S., Palanichamy, S., & Subramanian, G. (2010). Artemisia pallens as corrosion inhibitor for mild steel in HCl medium. *Materials Chemistry and Physics*, *120*(2), 643–648. https://doi.org/10.1016/j.matchemphys.2009.12.015

Karki, N., Neupane, S., Gupta, D. K., Das, A. K., Singh, S., Koju, G. M., Chaudhary, Y., & Yadav, A. P. (2021). Berberine isolated from *Mahonia nepalensis* as an eco-friendly and thermally stable corrosion inhibitor for mild steel in acid medium. *Arabian Journal of Chemistry*, *14*(12), 103423.

Khaled, K. F., & Abdel-Rehim, S. S. (2011). Electrochemical investigation of corrosion and corrosion inhibition of iron in hydrochloric acid solutions. *Arabian Journal of Chemistry*, *4*(4), 397–402. https://doi.org/10.1016/j.arabjc.2010.07.006

Koch, G., Varney, J., Thompson, N., Moghissi, O., Gould, M., & Payer, J. (2016). International measures of prevention, application, and economics of corrosion technologies study. *NACE International*, *216*, 2–3.

Kong, Z., Jin, Y., Sabbir Hossen, G. M., Hong, S., Wang, Y., Vu, Q.-V., Truong, V.-H., Tao, Q., & Kim, S.-E. (2022). Experimental and theoretical study on mechanical properties of mild steel after corrosion. *Ocean Engineering*, *246*, 110652. https://doi.org/10.1016/j.oceaneng.2022.110652

Laschuk, N. O., Easton, E. B., & Zenkina, O. V. (2021). Reducing the resistance for the use of electrochemical impedance spectroscopy analysis in materials chemistry. *RSC Advances*, *11*(45), 27925–27936.

Lasia, A. (2002). *Electrochemical impedance spectroscopy and its applications*.

Marsoul, A., Ijjaali, M., Elhajjaji, F., Taleb, M., Salim, R., & Boukir, A. (2020). Phytochemical screening, total phenolic and flavonoid methanolic extract of pomegranate bark (Punica granatum L): Evaluation of the inhibitory effect in acidic medium 1 M HCl. *Materials Today: Proceedings*, *27*, 3193–3198.

Mohamed, M. A., Jaafar, J., Ismail, A. F., Othman, M. H. D., & Rahman, M. A. (2017). Chapter 1—Fourier Transform Infrared (FTIR) Spectroscopy. In N. Hilal, A. F. Ismail, T. Matsuura, & D. Oatley-Radcliffe (Eds.), *Membrane Characterization* (pp. 3–29). https://doi.org/10.1016/B978-0-444-63776-5.00001-2

Mouanga, M., Andreatta, F., Druart, M.-E., Marin, E., Fedrizzi, L., & Olivier, M.-G. (2015). A localized approach to study the effect of cerium salts as cathodic inhibitor on iron/aluminum galvanic coupling. *Corrosion Science*, *90*, 491–502.

Nadi, I., Belattmania, Z., Sabour, B., Reani, A., Sahibed-dine, A., Jama, C., & Bentiss, F. (2019). *Sargassum muticum* extract based on alginate biopolymer as a new efficient biological corrosion inhibitor for carbon steel in hydrochloric acid pickling environment: Gravimetric, electrochemical and surface studies. *International Journal of Biological Macromolecules*, *141*, 137–149. https://doi.org/10.1016/j.ijbiomac.2019.08.253

Neha, P., Divya, L., & Nisha, S. (2015). Inhibition effect of *Hibiscus rosa* sinensis leaves extract on corrosion rate of Mild Steel in HCl medium. *International Journal of Research in Chemistry and Environment (IJRCE)*, *5*(3), 33–41.

Odewunmi, N. A., Umoren, S. A., Gasem, Z. M., Ganiyu, S. A., & Muhammad, Q. (2015). L-citrulline: An active corrosion inhibitor component of watermelon rind extract for mild steel in HCl medium. *Journal of the Taiwan Institute of Chemical Engineers*, *51*, 177–185.

Olasunkanmi, L. O., & Ebenso, E. E. (2020). Experimental and computational studies onpropanone derivatives of quinoxalin-6-yl-4,5-dihydropyrazole as inhibitors of mild steel corrosion in hydrochloric acid. *Journal of Colloid and Interface Science*, *561*, 104–116. https://doi.org/10.1016/j.jcis.2019.11.097

Ostovari, A., Hoseinieh, S. M., Peikari, M., Shadizadeh, S. R., & Hashemi, S. J. (2009). Corrosion inhibition of mild steel in 1M HCl solution by henna extract: A comparative study of the inhibition by henna and its constituents (Lawsone, Gallic acid, α-d-Glucose and Tannic acid). *Corrosion Science*, *51*(9), 1935–1949. https://doi.org/10.1016/j.corsci.2009.05.024

Palanisamy, G. (2019). Corrosion inhibitors. *Corrosion Inhibitors*, 1–24.

Parajuli, D., Sharma, S., Oli, H. B., Bohara, D. S., Bhattarai, D. P., Tiwari, A. P., & Yadav, A. P. (2022). Comparative Study of Corrosion Inhibition Efficacy of Alkaloid Extract of Artemesia vulgaris and Solanum tuberosum in Mild Steel

Samples in 1 M Sulphuric Acid. *Electrochem*, *3*(3), 416–433. https://doi.org/10.3390/electrochem3030029

Quraishi, M. A., Singh, A., Singh, V. K., Yadav, D. K., & Singh, A. K. (2010). Green approach to corrosion inhibition of mild steel in hydrochloric acid and sulphuric acid solutions by the extract of Murraya koenigii leaves. *Materials Chemistry and Physics*, *122*(1), 114–122. https://doi.org/10.1016/j.matchemphys.2010.02.066

Roberge, P. R. (2019). *Handbook of corrosion engineering*. McGraw-Hill Education.

Sadeghi Erami, R., Amirnasr, M., Meghdadi, S., Talebian, M., Farrokhpour, H., & Raeissi, K. (2019). Carboxamide derivatives as new corrosion inhibitors for mild steel protection in hydrochloric acid solution. *Corrosion Science*, *151*, 190–197. https://doi.org/10.1016/j.corsci.2019.02.019

Sharma, N., Khajuria, V., Gupta, S., Kumar, C., Sharma, A., Lone, N. A., Paul, S., Meena, S. R., Ahmed, Z., Satti, N. K., & Verma, M. K. (2021). Dereplication Based Strategy for Rapid Identification and Isolation of a Novel Anti-inflammatory Flavonoid by LCMS/MS from Colebrookea oppositifolia. *ACS Omega*, *6*(45), 30241–30259. https://doi.org/10.1021/acsomega.1c01837

Shrestha, P. R., Oli, H. B., Thapa, B., Chaudhary, Y., Gupta, D. K., Das, A. K., Nakarmi, K. B., Singh, S., Karki, N., & Yadav, A. P. (2019). Bark Extract of Lantana camara in 1M HCl as Green Corrosion Inhibitor for Mild Steel. *Engineering Journal*, *23*(4), 205–211. https://doi.org/10.4186/ej.2019.23.4.205

Tan, B., He, J., Zhang, S., Xu, C., Chen, S., Liu, H., & Li, W. (2021). Insight into anti-corrosion nature of Betel leaves water extracts as the novel and eco-friendly inhibitors. *Journal of Colloid and Interface Science*, *585*, 287–301. https://doi.org/10.1016/j.jcis.2020.11.059

Thapa Magar, J., Budhathoki, I. K., Rajaure, A., Oli, H. B., & Bhattarai, D. P. (2023). Alkaloid Extract of Ageratina adenophora Stem as Green Inhibitor for Mild Steel Corrosion in One Molar Sulfuric Acid Solution. *Electrochem*, *4*(1), 84–102. https://doi.org/10.3390/electrochem4010009

Thapa, O., Thapa Magar, J., Oli, H. B., Rajaure, A., Nepali, D., Bhattarai, D. P., & Mukhiya, T. (2022). Alkaloids of Solanum xanthocarpum Stem as Green Inhibitor for Mild Steel Corrosion in One Molar Sulphuric Acid Solution. *Electrochem*, *3*(4), 820–842. https://doi.org/10.3390/electrochem3040054

Touhami, F., Aouniti, A., Abed, Y., Hammouti, B., Kertit, S., Ramdani, A., & Elkacemi, K. (2000). Corrosion inhibition of armco iron in 1 M HCl media by new bipyrazolic derivatives. *Corrosion Science*, *42*(6), 929–940. https://doi.org/10.1016/S0010-938X(99)00123-7

Verma, C. (2021). *Handbook of science & engineering of green corrosion inhibitors: Modern theory, fundamentals & practical applications*. Elsevier.

Viswanatha, G. L., Shylaja, H., Kumar, H. Y., Venkataranganna, M., & Prasad, N. (2021). Traditional uses, phytochemistry, and ethnopharmacology of Colebrookea oppositifolia Smith: A mini-review. *Advances in Traditional Medicine*, *21*, 209–229.

Yamamoto, S., Abe, M., Tashiro, K., & Kawaoka, T. (2019). *A Novel Corrosion Rate Monitoring Method for Steel in Aqueous Solution Based on Tafel Extrapolation Method: Vol. All Days*.